# Stability and Hopf Bifurcation Analysis of a Rumor Propagation Model with Beddington-DeAngelis Incidence and Two Time Delays

Rongrong Yin, and Ahmadjan Muhammadhaji

***Abstract*—In this study, we investigated the dynamics of a delayed rumor propagation model with logistic growth and the Beddington-DeAngelis functional response. The model has two-time delays that describe the time required for the rumor propagation process and provide the existence conditions of the rumor equilibrium point. By applying the Lyapunov functional technique, we establish the necessary conditions for both the local and global asymptotic stability of the rumor equilibrium point. Moreover, we also analyze the local stability and Hopf bifurcation that arise as a result of time delay. In the context of a rumor propagation model with time delay, we introduce two control variables and subsequently derive the optimal solution through an optimization process. To further enhance our understanding of the system, we investigate the impact of a time delay on the equilibrium stability of the rumor propagation model using some numerical simulations.**

***Index Terms*—Beddington-DeAngelis functional response; Lyapunov functional; global stability; Hopf bifurcation**

## I. Introduction

WITH the advancement of science and technology, communication has become more accessible, but the channels for spreading rumors have also expanded, resulting in significant global consequences. In the information age, media play a central role in shaping public opinion. Particularly, the rapid growth of "we-media" platforms has become a major catalyst of rumors dissemination in recent years. Therefore, understanding the mechanisms and strategies underlying rumor transmission is essential for effectively controlling its spread and minimizing its potential harm.

Due to the striking similarities between the spread of rumors and transmission of infectious diseases, models originally designed for infectious disease propagation are commonly applied in rumor propagation research. Although both processes share similar characteristics, it is impossible to create a unified framework or an equivalent model for both. In 1965, Daley and Kendall [1] proposed a rumor propagation model, which assumes that individuals move between distinct groups according to a given probability distribution. They categorized the population into three groups: the ignorant, communicators, and rational individuals. Later, Maki and Murray [2] built upon the DK model through theoretical analysis, introducing an immune population and developing the MT rumor model. Subsequent research extended and refined the MT model [3-8]. For instance, Zhang et al. [9] addressed the limitations of the traditional SEIR model by considering trusted and questioned nodes, resulting in the SETQR model, which uses probability theory to describe the law of information propagation. Li et al. [10] examined the SIR model within the framework of logistic growth. Building on earlier work, Zhao et al. [11] modified the rumor propagation flowchart to enhance its realism and clarity. In another study, Zhao et al. [12] applied the SIR model for analytical and numerical studies of rumor spread within complex networks. To accurately represent real-world phenomena, time delays have also been incorporated into models [13-17]. Time lag is a well-known characteristic of real -world processes. In rumor propagation, delays may occur when users are unable to receive or disseminate a rumor promptly, resulting in a delay in information transmission. In [16], Zhang et al. improved the ILSR rumor propagation model by considering logistic growth and two discrete delays, addressing the Hopf bifurcation problem of positive equilibrium points in six distinct cases. In [17], Guo proposed a SEIMR model that incorporates media reports and time delays, analyzing the impact of media on rumor spread. The study revealed that the shorter the delay between media reports, the greater their influence and the more effectively they suppress rumors. These studies demonstrate the importance of real-world factors, such as government regulations and transmission delays, which are considered in the present study, in shaping in rumor propagation.

In [18], Li constructed a mathematical model that describes the basic dynamics of he interaction among the susceptible $S(t)$, propagating $I(t)$, and removing $R(t)$ individual as follows:

$$\begin{cases} \dfrac{dS}{dt} = rS(t)(1-\dfrac{S(t)}{K}) - \dfrac{\beta S(t)I(t)}{(1+\alpha_1 S(t))(1+\alpha_2 I(t))}, \\ \dfrac{dI}{dt} = \dfrac{\beta S(t-\tau_1)I(t-\tau_1)}{(1+\alpha_1 S(t-\tau))(1+\alpha_2 I(t-\tau))} - \mu I(t) \\ \qquad - \gamma(I(t)+R(t))I(t), \\ \dfrac{dR}{dt} = \gamma(I(t)+R(t))I(t) - \mu R(t). \end{cases} \tag{1}$$

Control strategies such as deleting rumor posts and educating the public on popular science were considered. To explore ways to control the spread of rumors, Li et

Manuscript received August 21, 2024; revised December 26, 2024.

This work was supported by the Open Project of Xinjiang Key Laboratory of Applied Mathematics (No. 2023D04045).

R. Yin is a postgraduate student of College of Mathematics and System Sciences, Xinjiang University, Urumqi 830017, P. R. China. (e-mail: 107552200661@stu.xju.edu.cn).

A. Muhammadhaji is an associate professor of College of Mathematics and System Sciences, Xinjiang University, Urumqi 830017, P. R. China. (Corresponding author to provide e-mail: ahmatjanam@aliyun.com).

al. [19] established an extended rumor propagation model, strengthened rumor identification and timely rumor-refuting education, and effectively controlled the spread of rumors. Jain et al. [20] introduced optimal control of rumor propagation in a uniformly mixed population. The above study shows that some practical factors need to be considered when rumors spread.

In [21], Miao et al. proposed a double-delay virus transmission model with Beddington-DeAngelis response and studied the dynamics of the considered model. As is known, the Beddington-DeAngelis functional response was proposed by Beddington et al.[22] and DeAngelis et al. [23]. In reality, rumor spreading is restricted by multiple factors. For example, resources such as people's attention and communication channels are limited. The Beddington-DeAngelis response function can take into account the competition for these limited resources among different roles like rumor spreaders and rumor refuters, making the model closer to the actual situation and accurately reflecting the resource constraints that rumors face during the spreading process. Moreover, it can describe the interactions among different groups, such as the complex relationships among rumor spreaders, susceptible individuals, and rumor refuters. The reflection of these interactions helps to gain a more comprehensive understanding of the dynamic process of rumor spreading and the roles played by different groups, thereby providing a basis for formulating more effective rumor control strategies. Therefore, we should introduce the Beddington-DeAngelis functional response into model foundation, which will have more resemblance to in reality. Based on the above discussions, in this paper, we consider the following system:

$$\begin{cases} \dfrac{dS(t)}{dt} = rS(t)(1-\dfrac{S(t)}{K}) - aS(t) - \dfrac{\beta S(t)I(t)}{1+\alpha S(t)+\lambda I(t)}, \\ \dfrac{dI(t)}{dt} = \dfrac{\beta e^{-m\tau_1}S(t-\tau_1)I(t-\tau_1)}{1+\alpha S(t-\tau_1)+\lambda I(t-\tau_1)} - (b+k)I(t), \\ \dfrac{dH(t)}{dt} = kI(t) - (c+\eta)H(t) + \varepsilon e^{-m\tau_2}R(t-\tau_2), \\ \dfrac{dR(t)}{dt} = \eta H(t) - dR(t) - \varepsilon e^{-m\tau_2}R(t-\tau_2), \end{cases} \tag{2}$$

where $S(t)$ denotes the ignorant crowd at time $t$, $I(t)$ denotes the spreading crowd at time $t$, $H(t)$ denotes the questioning crowd at time $t$, and $R(t)$ denotes the sober crowd at time $t$. $a>0,\ b>0,\ c>0$, and $d>0$ represent the mobility of rumors in the states of ignorance, propagation, suspicion, and awakening, respectively, and the condition that $r-a>0$ is satisfied; $\beta,\ k,\ \eta,\ K$, and $m$ are all positive constants. In addition, we have the following explanations for system (2):

(i) The increase in the ignorant population can be described by the mathematical model of population growth, which is represented by the formula $rS(1-\frac{S}{K})$. Here, $r$ indicates the population growth rate over time, $K$ represents the environmental population capacity, and all components do not exceed the environmental capacity.

(ii) In reality, a delay exists between initially hearing a rumor and spreading it, and we assume that rumor generation occurs after the rumor has passed a constant delay of $\tau_1$. $\tau_2$ is the time required for a doubter to think, verify, and become sober.

(iii) Constant $\varepsilon$ represents the doubt rate. When $\varepsilon>0$, then the sober person will be transferred to doubt at a rate of $\varepsilon$. When $\varepsilon=0$, then the sober person is unaffected by rumors and is always awake.

(iv) $\beta$ represents the transmission rate, while $k$ denotes the rate at which an individual transitions from a state of transmission to a state of questioning. $\eta$ represents the rate at which an individual transitions from questioning to awareness.

## II. Boundedness and Equilibrium Points

Let $\tau=\max\{\tau_1,\tau_2\}$, $R_+^4=\{(x_1,x_2,x_3,x_4): x_i\geq 0, i=1,2,3,4\}$ and $C([-\tau,0],R_+^4)$ be the space of continuous functions mapping the interval $[-\tau,0]$ into $R_+^4$ with the norm $\|\phi\|=\sup_{-\tau\leq t\leq 0}\{|\phi(t)|\}$ for any $\phi\in C([-\tau,0],R_+^4)$. The initial conditions for system (2) are given as follows

$$S(\theta)=\phi_1(\theta), I(\theta)=\phi_2(\theta), H(\theta)=\phi_3(\theta), R(\theta)=\phi_4(\theta),$$
$$\phi_i(\theta)\geq 0, \theta\in[-\tau,0]), \phi_i(0)>0 (i=1,2,3,4), \tag{3}$$

where $(\phi_1(\theta),\phi_2(\theta),\phi_3(\theta),\phi_4(\theta))\in C([-\tau,0],R_+^4)$ . It is well known by the fundamental theory of functional differential equation [24], system (2) admits a unique solution $(S(t),I(t),H(t),R(t))$ satisfying initial conditions (3).

**Theorem 2.1** The solutions of system (2) with initial condition (3) remain non-negative and ultimately bounded for all $t\geq 0$.

**Proof** According to [27] and [28], assume that $(S(t),I(t),H(t),R(t))$ be a solution of system (2) with initial condition (3) and defined on $[0,+\infty)$, let $\hat{m}=\min\{S(t),I(t),H(t),R(t)\}$, then $\hat{m}>0$. Assume that there exists $t^*>0$ such that $\hat{m}(t^*)=0$ and $\hat{m}(t)>0$ for all $t\in[0,t^*)$. If $\hat{m}(t^*)=S(t^*)$, from the first equation of model (2), we have

$$S(t^*)=S(0)e^{r(1-\frac{S(t^*)}{K})-a-\frac{\beta I(t^*)}{1+\alpha S(t^*)+\lambda I(t^*)}}>0,$$

which leads to a contradiction. Similarly, when $\hat{m}(t^*)=I(t^*)$, $\hat{m}(t^*)=H(t^*)$, and $\hat{m}(t^*)=R(t^*)$, we also can obtain the contradiction. Hence, $\hat{m}(t)>0$ for all $t\geq 0$, and thereby $(S(t),I(t),H(t),R(t))$ is positive for all $t\geq 0$.

Let $\mathcal{G}(t)=e^{-m\tau_1}S(t-\tau_1)+I(t)+H(t)+R(t)$ and $\gamma=\min\{a,b,c,d\}$. By positivity of $(S(t),I(t),H(t),R(t))$, we obtain

$$\begin{aligned} \dot{\mathcal{G}}(t) &= e^{-m\tau_1}rS(t-\tau_1)(1-\frac{S(t-\tau_1)}{K}) - (ae^{-m\tau_1}S(t- \\ &\quad \tau_1)+bI(t)+cH(t)+dR(t)) \\ &\leq e^{-m\tau_1}rK - (ae^{-m\tau_1}S(t-\tau_1)+bI(t)+cH(t) \\ &\quad +dR(t)) \\ &\leq e^{-m\tau_1}rK-\gamma\mathcal{G}(t). \end{aligned} \tag{4}$$

Thus we have,

$$\lim_{t\to\infty}\sup\mathcal{G}(t)\leq\frac{e^{-m\tau_1}}{\gamma}rK.$$

Therefore, all the solutions of system (2) are ultimately bounded.

The following is the basic regeneration number of system (2)

$$R_0=\frac{K\beta e^{-m\tau_1}(r-a)}{(b+k)[r+\alpha K(r-a)]}.$$

**Theorem 2.2** (i) System (2) has a trivial equilibrium point $E_0 = (0,0,0,0)$.

(ii) System (2) always has a rumor-free equilibrium point $E_1 = (\frac{K(r-a)}{r}, 0, 0, 0)$.

(iii) When $R_0 > 1$, then system (2) has a local equilibrium point $E_2 = (S_2, I_2, H_2, R_2,)$, where

$S_2 = \lambda K(r-a) + K[\alpha(b+k)e^{m\tau_1}] + K\sqrt{\Delta}$,
$I_2 = \frac{\beta S_2 - (b+k)(1+\alpha S_2)e^{m\tau_1}}{\lambda e^{m\tau_1}(b+k)}$,
$H_2 = \frac{k(d+\varepsilon e^{-m\tau_2})}{c(d+\varepsilon e^{-m\tau_2})+d\eta} I_2$,
$R_2 = \frac{\eta k}{c(d+\varepsilon e^{-m\tau_2})+d\eta} I_2$,
$\Delta = [\beta(1-\frac{1}{R_0}) + \frac{r\beta}{[r+\alpha K(r-a)]R_0} + \lambda(r-a)]^2 - 4\lambda(r-a)(1-\frac{1}{R_0})$.

## III. 3 Stability analysis Hopf bifurcations

In this section, we will examine the local and global asymptotic stability of equilibrium points $E_1$ and $E_2$ of system (2), in addition, we will obtain the conditions on the Hopf bifurcation.

### *3.1 Stability of equilibrium $E_1$*

**Theorem 3.1** In system (2), if $R_0 < 1$, then $E_1$ is locally asymptotically stable. If $R_0 > 1$, then $E_1$ is unstable.

**Proof** First, at equilibrium point $E_1$ of system (2), we can get the characteristic equation of the linearized system

$$[s-(a-r)](s+c+\eta)[s-(\frac{(r-a)K\beta e^{-(m+s)\tau_1}}{r+\alpha K(r-a)} - (b+k))][s+d+(1-\eta)\varepsilon e^{-(m+s)\tau_2}] = 0. \quad (5)$$

Then we have two roots $s_1, s_2$ of (5), where $s_1 = a-r < 0$, $s_2 = -(c+\eta) < 0$. When $\tau_1 = 0$, consider the following equation

$$s_3 - (\frac{(r-a)K\beta e^{-(m+s)\tau_1}}{r+\alpha K(r-a)} - (b+k)) = 0. \quad (6)$$

Then from (6) and the expression of $R_0$, we get $s_3 = (b+k)(R_0-1)$.

Clearly, when $R_0 < 1$, then $s_3 < 0$. In conclusion, when $\tau_1 = 0$, the rumor-free equilibrium point $E_1$ is locally asymptotically stable.

On the other hand, assume $s = i\omega$ with $\omega > 0$ be purely imaginary roots of (6), then we have

$$\omega = -\frac{(r-a)K\beta}{r+\alpha K(r-a)}\sin\omega\tau_1,$$

$$b+k = \frac{(r-a)K\beta}{r+\alpha K(r-a)}\cos\omega\tau_1,$$

which implies that $\omega^2 = (\frac{(r-a)K\beta}{r+\alpha K(r-a)})^2 - (b+k)^2$.

Note that when $R_0 < 1$, then $\omega^2 < 0$, which is a contradiction. In conclusion, equation (6) has no roots with non-negative real parts.

Now, we will consider the following equation

$$s + d + (1-\eta)\varepsilon e^{-(m+s)\tau_2} = 0. \quad (7)$$

When $\tau_2 = 0$, the above formula can be reduced to $s + d + (1-\eta)\varepsilon = 0$, then, we get $s = -d + (\eta - 1)\varepsilon < 0$. This indicates that the roots of equation (7) have negative real parts. By the general theory of the characteristic equation of delayed linear differential equation (see Kuang [27, Theorem 3.4.1]), if $R_0 < 1$, then $E_1$ is locally asymptotically stable. Next, if $R_0 > 1$, then let

$$f_1(s) = s - (\frac{(r-a)K\beta e^{-m\tau_1}}{r+\alpha K(r-a)} - (b+k)).$$

It is easy to see that

$$f_1(0) = b+k-\frac{(r-a)K\beta e^{-(m+s)\tau_1}}{r+\alpha K(r-a)} = (b+k)(1-R_0) < 0,$$

and

$$\lim_{s\to+\infty} f_1(s) = +\infty.$$

Thus, $f(s) = 0$ has at least one positive real root. Hence, if $R_0 > 1$, then equilibrium point $E_1$ of system (2) is unstable. This completes the proof.

**Theorem 3.2** The rumor-free equilibrium point $E_1$ of system (2) is globally asymptotically stable if $R_0 \leq 1$.

**Proof** Define Lyapunov functional $V_1(t)$ as follows

$$V_1(t) = S(t) - S_1 - S_1 \ln\frac{S_1}{S(t)} + e^{m\tau_1}I(t) + H(t) + R(t) + U^-(t),$$

where $U^-(t) = \int_t^{t-\tau_1} \frac{\beta S(\theta)I(\theta)}{1+\alpha S(\theta)+\lambda I(\theta)} d\theta$. Calculating the derivative of $V_1(t)$ along with any positive solution of system (2) and from $S_1 = \frac{K(r-a)}{r}$, we can obtain

$$\begin{aligned}\frac{dV_1(t)}{dt} \leq& -\frac{(S-S_1)^2}{K} + \frac{\beta S_1 I(t)}{1+\alpha S(t)+\lambda I(t)} + kI(t) \\ &- (b+k)e^{m\tau_1}I(t) - cH(t) - dR(t) \\ =& -\frac{(S-S_1)^2}{K} + \frac{\beta K(r-a)I(t)}{r(1+\alpha S(t)+\lambda I(t))} \\ &- (b+k)e^{m\tau_1}I(t) + kI(t) - cH(t) - dR(t) \\ \leq& -\frac{(S-S_1)^2}{K} + \frac{e^{m\tau_1}(b+k)(1+\alpha S_1)}{1+\alpha S(t)+\lambda I(t)}(R_0-1) - \\ &e^{m\tau_1}I(t) - kI(t)(e^{m\tau_1}-1) - cH(t) - dR(t).\end{aligned}$$

Obviously, if $R_0 \leq 1$, then $\frac{dV_1(t)}{dt} \leq 0$ for any $(S(t), I(t), H(t), R(t))$. We have $\frac{dV_1(t)}{dt} = 0$ if and only if $S = S_1, I = 0, H = 0, R = 0$. Let $N$ be the largest invariant set of $\{(S(t), I(t), H(t), R(t)) \in R_4^+ : \frac{dV_1}{dt} = 0\}$. We easily obtain $N = \{E_1\}$. According to LaSalle's invariance principle [27], equilibrium $E_1$ of system (2) is globally asymptotically stable if $R_0 \leq 1$. This completes the proof.

### *3.2 Stability of equilibrium point $E_2$*

In this subsection, we will discuss the local and global asymptotic stability of equilibrium point $E_2$ for the cases of $\tau_1 \geq 0$ and $\tau_2$ = 0.

At equilibrium point $E_2$, we can get the following characteristic equation of the corresponding linearized system of system (2)

$$\begin{aligned}&[(s+c+\eta)(s+d+\varepsilon e^{-(m+s)\tau_2}) - \eta\varepsilon e^{-(m+s)\tau_2}]\times \\ &[(s - r(1-\frac{2S_2}{K}) + a + A_2)(s - B_2 e^{-(m+s)\tau_1} + b + k) + \\ &A_2 B_2 e^{-(m+s)\tau_1}] = 0,\end{aligned} \quad (8)$$

where

$$A_2 = \frac{\beta I_2(1+\lambda I_2)}{(1+\alpha S_2+\lambda I_2)^2}, \qquad B_2 = \frac{\beta S_2(1+\alpha S_2)}{(1+\alpha S_2+\lambda I_2)^2}.$$

First, we discuss the local asymptotic stability of equilibrium point $E_2$

**Theorem 3.3** If $\tau_1 \geq 0,\ \tau_2 = 0$ and $R_0 > 1$, then equilibrium point $E_2$ is locally asymptotically stable.

**Proof** When $\tau_2 = 0$, the characteristic equation can be written as

$$[(s+c+\eta)(s+d+\varepsilon)-\eta\varepsilon][(s-r(1-\frac{2S_2}{K})+a+A_2)\times (s-B_2e^{-(m+s)\tau_1}+b+k)+A_2B_2e^{-(m+s)\tau_1}]=0.$$

First consider the equation: $(s+c+\eta)(s+d+\varepsilon)-\eta\varepsilon=0$, that is

$$s^2+(c+d+\eta+\varepsilon)s+cd+c\varepsilon+\eta d=0. \tag{9}$$

Since

$$s_1+s_2=-(c+d+\eta+\varepsilon)<0 \quad \text{and} \quad s_1s_2=cd+c\varepsilon+\eta d>0.$$

Then by the Routh-Hurwitz criterion, all roots of (9) have negative real parts.

Next consider the equation:

$$(s-r(1-\frac{2S_2}{K})+a+A_2)(s-B_2e^{-(m+s)\tau_1}+b+k) + A_2B_2e^{-(m+s)\tau_1}=0.$$

By using

$$e^{-m\tau_1}=\frac{(b+k)(1+\alpha S_2+\lambda I_2)}{\beta S_2I_2},$$
$$(b+k)I_2=\frac{\beta e^{-m\tau_1}S_2I_2}{1+\alpha S_2+\lambda I_2},$$
$$e^{-m\tau_2}=\frac{\eta H_2-dR_2}{\varepsilon R_2}.$$

Then, from the above formula we get

$$(s+b+k)[s-r(1-\frac{2S_2}{K})+a+A_2] =\frac{(1+\alpha S_2)(b+k)e^{-s\tau_1}}{1+\alpha S_2+\lambda I_2}[s-r(1-\frac{2S_2}{K})+a]. \tag{10}$$

Assume that equation (10) has a non-negative real root $s$, where $s=\alpha_0+i\omega_0$ with $\alpha_0\geq 0,\ \omega_0\geq 0$.

$$(\alpha_0+i\omega_0+b+k)[\alpha_0+i\omega_0-r(1-\frac{2S_2}{K})+a+A_2] =\frac{(1+\alpha S_2)(b+k)e^{-(\alpha_0+i\omega_0)\tau_1}}{1+\alpha S_2+\lambda I_2}[\alpha_0+i\omega_0-r(1-\frac{2S_2}{K}) +a]. \tag{11}$$

Since

$$|\alpha_0+i\omega_0+b+k|^2=\alpha_0^2+2(b+k)(\alpha_0+i\omega_0)+(b+k)^2 \geq (\frac{(1+\alpha S_2)(b+k)}{1+\alpha S_2+\lambda I_2})^2,$$

and

$$\alpha_0+i\omega_0+b+k\geq \frac{(1+\alpha S_2)(b+k)}{1+\alpha S_2+\lambda I_2},$$

then, we have

$$\alpha_0+i\omega_0-r(1-\frac{2S_2}{K})+a+A_2\geq \alpha_0+i\omega_0-r(1-\frac{2S_2}{K})+a.$$

By analyzing the left and right hand side of (11), we can see a contradiction. Consequently, it can be found that the characteristic equation (10) has no roots with a nonnegative real part. As a result, under the conditions $\tau_1\geq 0,\ \tau_2=0$ and $R_0>1$, equilibrium point $E_2$ of system (2) is locally asymptotically stable. This completes the proof.

**Theorem 3.4** If $\tau_1 \geq 0,\ \tau_2 = 0$ and $R_0 > 1$, then equilibrium point $E_2$ is globally asymptotically stable.

**Proof** It is clear that in order to prove that equilibrium point $E_2$ of system (2) is locally asymptotically stable, we only need to prove that the following system is globally asymptotically stable

$$\begin{cases} \dfrac{dS(t)}{dt}=rS(t)(1-\dfrac{S(t)}{K})-aS(t)-\dfrac{\beta S(t)I(t)}{1+\alpha S(t)+\lambda I(t)},\\ \dfrac{dI(t)}{dt}=\dfrac{\beta e^{-m\tau_1}S(t-\tau_1)I(t-\tau_1)}{1+\alpha S(t-\tau_1)+\lambda I(t-\tau_1)}-(b+k)I(t). \end{cases}$$

Define a Lyapunov functional as follows.

$$V_2=(S(t)-S^*-S^*\ln\frac{S(t)}{S^*})e^{-m\tau_1}+I(t)-I^*-I^*\ln\frac{I(t)}{I^*}.$$

Now, we calculate the derivative of $V(t)$ along with the solution of system (2).

$$\begin{aligned}
\frac{dV_2}{dt}&=e^{-m\tau_1}[rS(t)(1-\frac{S(t)}{K})-\frac{\beta e^{-m\tau_1}S(t)I(t)}{1+\alpha S(t)+\lambda I(t)}\\
&\quad -a(S(t)-S^*)-rS^*(1-\frac{S(t)}{K})+\\
&\quad \frac{\beta S^*I(t)}{1+\alpha S(t)+\lambda I(t)}]+\frac{\beta e^{-m\tau_1}S(t)I(t)}{1+\alpha S(t)+\lambda I(t)}-\\
&\quad (b+k)I(t)-\frac{\beta e^{-m\tau_1}S(t)I^*}{1+\alpha S(t)+\lambda I(t)}+(b+k)I^*\\
&=(S^*-S)(r-a)e^{-m\tau_1}-(S-S^*)\frac{rS}{K}e^{-m\tau_1}\\
&\quad -(b+k)(I-I^*)-\frac{\beta e^{-m\tau_1}}{1+\alpha S+\lambda I}(SI^*-S^*I)\\
&=(a-r)(S^*-S)-\frac{rS}{K}(S-S^*)-(b+k)(I-I^*)\\
&\quad -\frac{\beta e^{-m\tau_1}}{1+\alpha S+\lambda I}(SI^*-S^*I)\\
&\leq (a-r)(S^*-S)^2-\frac{r}{K}(S-S^*)^2-(b+k)(I-I^*)\\
&\quad -\frac{\beta e^{-m\tau_1}}{1+\alpha S+\lambda I}(SI^*-S^*I)\\
&=(a-r-\frac{r}{K})(S^*-S)^2e^{-m\tau_1}-(b+k)(I-I^*)\\
&\quad -\frac{\beta e^{-m\tau_1}}{1+\alpha S+\lambda I}(SI^*-S^*I)\\
&=(a-r-\frac{r}{K})(S^*-S)^2e^{-m\tau_1}-(b+k)(I-I^*)\\
&\quad -\frac{\beta e^{-m\tau_1}}{1+\alpha S+\lambda I}SI^*+\frac{\beta e^{-m\tau_1}S^*I}{1+\alpha S+\lambda I}\\
&=(b+k)I[\frac{a-r-\frac{r}{K}}{b+k}(S-S^*)^2e^{-m\tau_1}-1+\frac{I^*}{I}\\
&\quad -\frac{\beta e^{-m\tau_1}SI^*}{I(b+k)(1+\alpha S+\lambda I)}+\frac{\beta e^{-m\tau_1}S^*}{(b+k)(1+\alpha S+\lambda I)}]\\
&\leq (b+k)I[\frac{a-r-\frac{r}{K}}{b+k}(S-S^*)^2e^{-m\tau_1}-(1+\lambda I)\\
&\quad \times(R_0-1)\frac{I^*}{I}].
\end{aligned}$$

Obviously, if $R_0>1$, then $\frac{dV_2}{dt}\leq 0$ for any $(S(t),I(t))$. We have $\frac{dV_2}{dt}=0$ if and only if $S=S^*$, and $I=I^*$. According to Lasalle's invariance principle, $E_2$ is globally asymptotically stable.

*3.3. Hopf bifurcation analysis*

From characteristic equation (8), we have

$$s^4+e_3s^3+e_2s^2+e_1s+e_0+(h_3s^3+h_2s^2+h_1s+h_0)e^{-s\tau_1}=0, \quad (12)$$

where

$$\begin{aligned}
e_3 &= a+b+c+d+\eta+k+A_2-B_2-r(1-\frac{2S_2}{K}),\\
e_2 &=(c+\eta)d+a+b+k+A_2-r(1-\frac{2S_2}{K})\\
&\quad+(r(1-\frac{2S_2}{K})+a)B_2+[a+b+k+A_2-B_2\\
&\quad-r(1-\frac{2S_2}{K})](c+d+\eta),\\
e_1 &=(c+\eta+d)[a+b+k+A_2-r(1-\frac{2S_2}{K})\\
&\quad+(r(1-\frac{2S_2}{K})+a)B_2]+[a+b+k+A_2-B_2\\
&\quad-r(1-\frac{2S_2}{K}](c+\eta)d,\\
e_0 &=d(c+\eta)[a+b+k+A_2-r(1-\frac{2S_2}{K})+(r(1-\\
&\quad\frac{2S_2}{K})+a)B_2],\\
h_3 &= \varepsilon\xi, \quad \xi=\frac{\eta H_2-dR_2}{\varepsilon R_2},\\
h_2 &= [a+b+c+k+A_2-B_2-r(1-\frac{2S_2}{K})]\varepsilon\xi,\\
h_1 &=[a+b+k+A_2-r(1-\frac{2S_2}{K})+(r(1-\frac{2S_2}{K})+a)\times\\
&\quad B_2]\varepsilon\xi+[a+b+k+A_2-B_2-r(1-\frac{2S_2}{K})]c\varepsilon\xi,\\
h_0 &=[a+b+k+A_2-r(1-\frac{2S_2}{K})+(r(1-\frac{2S_2}{K})+a)\times\\
&\quad B_2]c\varepsilon\xi,
\end{aligned}$$

where $e_k,\ h_l \in \mathbb{R}\ (k,l=0,1,2,3)$ are all real constants and $\sum_0^3 h_l^2 \neq 0$.

Next, from equation (12) with $\tau_1=0$, we have

$$s^4+(e_3+h_3)s^3+(e_2+h_2)s^2+(e_1+h_1)s+e_0+h_0=0. \quad (13)$$

Theorem 3.3 indicates that all roots of equation (13) have negative real parts.

Clearly, when $\tau_1>0$, $s=i\omega(\omega>0)$ is a root of the equation (12), then we have

$$\begin{aligned}
&\omega^4+ie_3\omega^3-e_2\omega^2+ie_1\omega+e_0+(-ih_3\omega^3-h_2\omega^2\\
&+ih_1\omega+h_0)(\cos\omega\tau-i\sin\omega\tau)=0.
\end{aligned}$$

From the above equation, we further obtain

$$\begin{aligned}
\omega^4-e_2\omega^2+e_0&=(h_2\omega^2-h_0)\cos\omega\tau_1+(h_3\omega^3-h_1\omega)\sin\omega\tau_1,\\
-e_3\omega^3+e_1\omega&=(h_3\omega^3-h_1\omega)\cos\omega\tau_1-(h_2\omega^2-h_0)\sin\omega\tau_1.
\end{aligned} \quad (14)$$

Then it follows from (14)

$$\omega^8+u\omega^6+v\omega^4+m\omega^2+g_0=0, \quad (15)$$

where

$$u=e_3^2-2e_2-h_3^2, \qquad m=e_1^2-2e_0e_2+2h_0h_2-h_1^2,$$

$$v=e_2^2+2e_0-2h_1e_3-h_2^2+2h_1h_3, \qquad g_0=e_0^2-h_0^2.$$

Let $x=\omega^2$, then from (15) we have

$$x^4+ux^3+vx^2+mx+g_0=0. \quad (16)$$

Suppose that

$$F(x)=x^4+ux^3+vx^2+mx+g_0, \quad (17)$$

then we have the following Lemma.

**Lemma 3.1** If $g_0<0$, then equation (16) has at least one positive root.

**Proof** Clearly, $F(0)=g_0<0$, and $\lim_{x\to\infty}F(x)=\infty$. Hence, there exists a $x_0\in(0,\infty)$ so that $F(x_0)=0$. This completes the proof.

In order to obtain the next lemma, we need to discuss the following differential equation.

From (17), we have

$$\frac{dF(x)}{dx}=4x^3+3ux^2+2vx+m=4f(x),$$

where

$$f(x)=x^3+\frac{3}{4}ux^2+\frac{1}{2}vx+\frac{1}{4}m. \quad (18)$$

Let

$$p=\frac{v}{2}-\frac{3}{16}u^2, \quad q=\frac{1}{32}u^3-\frac{1}{8}uv+m, \quad \wp=\frac{q^2}{4}+\frac{p^3}{27}.$$

Then from [24], we can obtain the following results on the distribution of roots of equation (17).

$$\begin{aligned}
&\text{if } \wp>0, \quad x_1^*=-\frac{u}{4}+\sqrt[3]{-\frac{q}{2}+\sqrt{\wp}}+\sqrt[3]{-\frac{q}{2}-\sqrt{\wp}},\\
&\text{if } \wp=0, \quad x_2^*=\max\{-\frac{u}{4}-2\sqrt[3]{-\frac{q}{2}},\ -\frac{u}{4}+2\sqrt[3]{-\frac{q}{2}}\},\\
&\text{if } \wp=0, \quad x_3^*=\max\big\{-\frac{u}{4}+2\,\mathrm{Re}\{\delta\},-\frac{u}{4}+2\,\mathrm{Re}\{\delta\epsilon\},\\
&\qquad\qquad -\frac{u}{4}+2\,\mathrm{Re}\{\delta\bar{\epsilon}\}\big\},
\end{aligned}$$

where $\delta$ is one of cube roots of the complex number $-\frac{q}{2}+\sqrt{\wp}$ and $\epsilon=-\frac{1}{2}+\frac{\sqrt{3}}{2}i$. By making a similar argument as [27], we obtain the following results.

**Lemma 3.2** If $g_0\geq 0$ , then equation (17) has no positive root if one of the following conditions holds:

(i) $\wp>0$ and $x_1^*<0$ ;
(ii) $\wp=0$ and $x_2^*<0$ ;
(iii) $\wp<0$ and $x_3^*<0$ .

**Lemma 3.3** If $g_0\geq 0$, then equation (17) has at least one positive root if one of the following conditions holds:

(i) $\wp>0,\ x_1^*>0$ and $F(x_1^*)<0$;
(ii) $\wp=0,\ x_2^*>0$ and $F(x_2^*)<0$ ;
(iii) $\wp<0,\ x_3^*>0$ and $F(x_3^*)<0$ .

**Proof** (i) If $\wp>0$, we know that formula (18) has a unique real root $x_1$, that is, formula (17) also has a unique real root $x_1$. Since $F(x)$ is differentiable, and $\lim_{x\to\infty}F(x)=\infty$, we know that $x_1$ is the unique stagnation point and minimum point of $F(x)$. This is obvious.

Now,we just need to prove it's necessary. We assume that $x_1\leq 0$ or $x_1>0$ has $F(x_1)>0$. If $x_1\leq 0$, since $F(0)=g_0>0$ is the minimum of $F(x)$, so $F(x)$ has no positive real zero. If $x_1>0$, and $F(x)>0$, since $\min_{x>0}\{F(x)\}=F(x_1)>0$, it follows that $F(x)$ has no positive real root. Next, the proof of case (ii) is similar to the previous case (i).

(iii) Without losing its generality, we suppose that the equation (17) has $n$ positive roots and $n\in\{1,2,3,4\}$, denoted by $x_k^*, k=1,2,\cdots n$. Then the equation (15) has $n$ positive roots, denoted by $\omega_k=\sqrt{x_k^*},\ k=1,2,\cdots n$.

By equation (14) we have

$$\sin \omega\tau_1 = \frac{\hbar_1}{\hbar}, \tag{19}$$

where

$$\begin{aligned}\hbar_1 =&(\omega^4 - e_2\omega^2 + e_0)\left(h_3\omega^3 - h_1\omega\right)\\ &+ (e_3\omega^3 - e_1\omega)(h_2\omega^2 - h_0),\\ \hbar =& (h_3\omega^3 - h_1\omega)^2 + (h_2\omega^2 - h_0)^2.\end{aligned}$$

When $\omega = \omega_k (k = 1, 2, \cdots, n)$ , from (19) we have

$$\tau_k^{(j)} = \frac{1}{\omega_k}\arcsin(\frac{\hbar_1}{\hbar}) + \frac{2\pi j}{\omega_k},$$

where $k = 1, 2, \cdots, n, \quad j = 0, 1, \cdots$. Thus, when $\tau = \tau_k^{(j)}, k = 1, 2, \cdots, n, \ j = 0, 1, \cdots, \pm i\omega_k$ is a pair of purely imaginary roots of the equation (13). Clearly, for every $k = 1, 2, \cdots, n, \ \left\{\tau_k^{(j)}\right\}$ is monotonically increasing for $j = 0, 1, 2, \cdots$ and

$$\lim_{j\to+\infty} \tau_k^{(j)} = \infty.$$

Therefore, there is a $k_0 \in \{1, 2, \cdots, n\}$ and $j_0 \in \{0, 1, 2, \cdots\}$ such that

$$\tau_0 = \tau_{k_0}^{(j_0)} = \min\left\{\tau_k^{(j)} : k = 1, 2, \cdots, n, \ j = 0, 1, 2, \cdots\right\}.$$

Thus, we can define

$$\omega_0 = \omega_{k_0}, \quad x_0 = x_{k_0}^*. \tag{20}$$

Let $s(\tau_1) = \rho(\tau_1) + i\omega(\tau_1)$ be a root of equation (12) and satisfying

$$\rho(\tau_0) = 0, \quad \omega(\tau_0) = \omega_0.$$

It is easy to get the distribution of roots of equation (12).

**Lemma 3.4** For equation (12), the following states are true:
(i)If $g_0 \geq 0$ , and one of the following conditions holds:
(a) $\wp > 0$ and $x_1^* < 0$ ;
(b) $\wp = 0$ and $x_2^* < 0$ ;
(c) $\wp < 0$ and $x_3^* < 0$ .
(ii)If $g_0 < 0$ or $g_0 \geq 0$, and one of the following conditions is true:
(a) $\wp > 0, \ x_1^* > 0$ and $F(x_1^*) < 0$;
(b) $\wp = 0, \ x_2^* > 0$ and $F(x_2^*) < 0$ ;
(c) $\wp < 0, \ x_3^* > 0$ and $F(x_3^*) < 0$ .

**Lemma 3.5** Suppose that $x_k = \omega_k^2$ and $\frac{dx_k}{dx} \neq 0$. Then the following conditions of transversality hold:

$$Re[\frac{dx_k(\tau)}{d\tau}|_{\tau=\tau_k^j}] \neq 0,$$

and the sign $Re[\frac{dx_k(\tau)}{d\tau}|_{\tau=\tau_k^j}]$ is the same as that of $\frac{dF(x_k)}{dx}$.

**Proof** Differentiating equation (12) with respect to $\tau_1$, we get

$$\begin{aligned}&(4s^3 + 3e_3s^2 + 2e_2s + e_1)\frac{ds}{d\tau_1} + (3h_3s^2 + 2h_2s + h_1)\times\\ &e^{-s\tau_1}\frac{ds}{d\tau_1} + (h_3s^3 + h_2s^2 + h_1s + h_0)(-s - \tau_1\frac{ds}{d\tau_1})e^{-s\tau_1}\\ &= 0,\end{aligned}$$

and

$$\begin{aligned}(\frac{ds}{d\tau_1})^{-1} =& -\frac{4s^3 + 3e_3s^2 + 2e_2s + e_1}{s(s^4 + e_3s^3 + e_2s^2 + e_1s + e_0)}\\ &+ \frac{3h_3s^2 + 2h_2s + h_1}{s(h_3s^3 + h_2s^2 + h_1s + h_0)} - \frac{\tau_1}{s}.\end{aligned}$$

Therefore

$$\begin{aligned}&\text{sign}\left\{\frac{d\,\text{Re}(s(\tau_1))}{d\tau_2}\right\}\Big|_{\tau_1=\tau_k^{(j)}} = \text{sign}\left\{\text{Re}\left(\frac{ds}{d\tau_1}\right)^{-1}\right\}\Big|_{s=i\omega_0}\\ &= \text{sign}\{\frac{4\omega_0^6+\omega_0^4\left(3e_3^2-6e_2\right)+\omega_0^2\left(-4e_3e_1+4e_0+2e_2^2\right)+\left(e_1^2-2e_2e_0\right)}{\omega_0^2\left(e_3\omega_0^2-e_1\right)^2+\left(\omega_0^4-e_2\omega_0^2+e_0\right)^2}\\ &\quad+\frac{-3h_3^2\omega_0^4+\omega_0^2\left(4h_1h_3-2h_2^2\right)+\left(-h_1^2+2h_2h_0\right)}{\omega_0^2\left(h_3\omega_0^2-h_1\right)^2+\left(h_2\omega_0^2-h_0\right)^2}\}.\end{aligned}$$

From equation (15), we get

$$\begin{aligned}&\omega_0^2\left(e_3\omega_0^2 - e_1\right)^2 + \left(\omega_0^4 - e_2\omega_0^2 + e_0\right)^2\\ &= \omega_0^2\left(e_3\omega_0^2 - h_1\right)^2 + \left(h_2\omega_0^2 - h_0\right)^2.\end{aligned}$$

Therefore, we have

$$\begin{aligned}&\text{sign}\left\{\frac{d\,\text{Re}\left(s\left(\tau_1\right)\right)}{d\tau_1}\right\}\Big|_{\tau_2=\tau_k^{(j)}}\\ &= \text{sign}\left[\frac{F'\left(x_k\right)}{\left(h_3\omega_0^2 - h_1\right)^2\omega_0^2 + \left(h_0 - h_2\omega_0^2\right)^2}\right].\end{aligned}$$

Since $x_k > 0$ , we obtain that $\frac{d\,\text{Re}(s(\tau_1))}{d\tau_1}\Big|_{\tau_1=\tau_k^{(j)}}$ and $F'\left(x_k\right)$ have the same sign. Therefore, we finally have the following result.

**Theorem 3.5** Let $\tau_0$, $\omega_0$ and $x_0$ be defined by (19). Then we can draw the following conclusions:

(i) If equation (17) possesses no positive real roots, then the equilibrium point $E_2$ is locally asymptotically stable for any $\tau_1 \geq 0$.

(ii) If equation (17) possesses $n$ positive real roots, then equilibrium $E_2$ is locally asymptotically stable for $\tau_1 \in [0, \tau_0)$.

(iii) Assume $x_0$ is a simple root of $F(x) = 0$ , then there is a Hopf bifurcation for system (2) at the equilibrium $E_2$ as $\tau_1$ surpass the critical value $\tau_0$.

**Proof** According to equation (20), we can easily have conclusions of (i) and (ii); therefore, we only need to prove conclusion (iii). Since $x_0$ is a simple root of (17), we know $F(x_0) \neq 0$. If $F'\left(x_0\right) < 0$, then the characteristic equation (12) has at least a root with positive real part when $\tau_1$ is slightly less than $\tau_0$. It will lead to a contradiction with conclusion (ii) in Theorem 3.5. Therefore, we have $F'\left(x_0\right) > 0$. This implies the existence of a Hopf bifurcation of model (2). This completes the proof.

## IV. Persistence of the system

Our interest of this section, is to establish the conditions for the persistence of system (2) with initial condition (3), by applying the method given in [25,26], we show the persistence of system (2) for $R_0 > 1$. This result shows that the rumor eventually persistence for $R_0 > 1$.

**Theorem 4.1** If $R_0 > 1$, system (2) is weakly persistent.

**Proof** According to Theorem 3.1, there is a positive orbit $(S(t), I(t), H(t), R(t))$ of system (2) such that.

$$\lim_{t\to\infty}\sup S(t) = \frac{K(r-a)}{r}, \qquad \lim_{t\to\infty}\sup I(t) = 0,$$

$$\lim_{t\to\infty}\sup H(t) = 0, \qquad \lim_{t\to\infty}\sup R(t) = 0.$$

There exists a sufficiently small quantity $\eth > 0$, then

$$(r-a)\beta e^{-m\tau_1} > \frac{(b+k)[r + \alpha(K-\eth)(r-a)]}{K-\eth}$$

Next, we can consider,

$$\begin{aligned} \dot{u_1}(t) &= \frac{\beta e^{-m\tau_1}(K-ð)(r-a)u_1}{r+\alpha(K-ð)(r-a)+r\lambda u_1}-(b+k)u_1,\\ \dot{v_1}(t) &= ku_1-(c+\eta)v_1+\varepsilon e^{-m\tau_2}z_1,\\ \dot{z_1}(t) &= \eta v_1 - dz_1-\varepsilon e^{-m\tau_2}z_1. \end{aligned} \tag{21}$$

For a sufficiently large $T>0$, when $t>T$, the equation can then be formulated as:

$$\begin{aligned} \dot{I}(t) &= \frac{\beta e^{-m\tau_1}(K-ð)(r-a)I}{r+\alpha(K-ð)(r-a)+r\lambda I}-(b+k)I,\\ \dot{H}(t) &= kS-(c+\eta)I+\varepsilon e^{-m\tau_2}R,\\ \dot{R}(t) &= \eta H - dR-\varepsilon e^{-m\tau_2}R. \end{aligned}$$

Through $E(0,0,0)$ and $E^*(u^*,v^*,z^*)$, the equilibrium points of equation (21) can be obtained

$$\begin{aligned} u_1^* &= \frac{\beta e^{-m\tau_2}(K-ð)(r-a)}{r\lambda(b+k)}-\frac{r+\alpha(K-ð)(r-a)}{r\lambda},\\ v_1^* &= \frac{k(d+\varepsilon e^{-m\tau_2})}{d(c+\eta)+c\varepsilon e^{-m\tau_2}}u_1^*,\\ z_1^* &= \frac{\eta}{d+\varepsilon e^{-m\tau_2}}v_1^*. \end{aligned}$$

The variational matrix corresponding to equation (21) is provided by the expression below:

$$V_ð=\begin{bmatrix}\beta^* & 0 & 0\\ k & -(c+\eta) & \varepsilon e^{-m\tau_2}\\ 0 & \eta & -(d+\varepsilon e^{-m\tau_2})\end{bmatrix},$$

where $\beta^*=\frac{\beta e^{-m\tau_1}(K-ð)(r-a)[r+\alpha(K-ð)(r-a)]}{[r+\alpha(K-ð)(r-a)+r\lambda u_1^*]^2}-(b+k)$.

It can be noticed from the variational matrix $V_ð$ that the off-diagonal elements are all non-negative. According to the stipulations of the Perron-Frobenius theorem, a non-negative eigenvector $z_1(z_1^1;\, z_1^2;\, z_1^3)$ pertains to the maximum root $\widetilde{x_1}$ of the variational matrix $V_ð$. The characteristic polynomial of $V_ð$ is expressed as:

$$\begin{aligned} &s^3+s^2(c+d+\eta+\varepsilon e^{-m\tau_2}-\beta^*)+[(c+\eta)(d+\varepsilon e^{-m\tau_2})\\ &-(c+d+\eta+\varepsilon e^{-m\tau_2})]s-(c+\eta)(d+\varepsilon e^{-m\tau_2})\beta^*\\ &-\eta\varepsilon e^{-m\tau_2}=0. \end{aligned}$$

The above polynomial is of degree three, so it has three roots. According to Vieta's formulas, we can obtain that

$$\widetilde{x_1}\cdot\widetilde{x_2}\cdot\widetilde{x_3}=(c+\eta)(d+\varepsilon e^{-m\tau_2})\beta^*+\eta\varepsilon e^{-m\tau_2}>0.$$

It can be analyzed that equation (21) has at least one positive root, which is denoted as $\widetilde{x_1}>0$. Suppose that when $t=T$, $z_1(t)=(z_1^1(t),z_1^2(t),z_1^3(t))$ is the solution of equation (21) towards $(l_1z_1^1,l_2z_1^2,l_3z_1^3)$, where length $l_i>0, i=1,2,3$ satisfies the conditions, $l_1z_1^1<I(t)$, $l_2z_1^2<H(t)$, $l_3z_1^3<R(t)$.

Apparently,

$$\begin{bmatrix}u_1\\ v_1\\ z_1\end{bmatrix}=\begin{bmatrix}l_1z_1^1e^{\widetilde{x_1}t}\\ l_2z_1^2e^{\widetilde{x_1}t}\\ l_3z_1^3e^{\widetilde{x_1}t}\end{bmatrix}.$$

$u_1(t), v_1(t)$ and $z_1(t)$ are strictly increasing function of $t$ , also $(u_1(t),v_1(t),z_1(t))\to+\infty$ , as $t\to+\infty$ . Hence, $(I(t),H(t),R(t))\to+\infty$ for $t\to+\infty$, which oppose the fact that $\lim_{t\to+\infty}I(t)=0$, $\lim_{t\to+\infty}H(t)=0$ and $\lim_{t\to+\infty}R(t)=0$. Therefore, no positive orbit for the system (2) tends to $(\frac{K(r-a)}{r},0,0)$ as $t\to+\infty$. Consequently, this shows that system (2) is weakly persistent. Hence, this completes the proof.

## V. Optimal Control

If the spread of rumors is not checked, it will have a serious impact on social order, public security, and national image. For instance, during nuclear leaks in Japan, several Chinese people believed that salt production would be affected; consequently, they frantically bought and stored iodized salt, leading to social panic and salt shortages. Therefore, to reduce their spread, controlling rumors is essential. To this end, we introduce two time-controlled variables, $p_1$ and $p_2$, which represent cost controls to reduce the probability of rumor spreading and the strength of avoiding or removing posts through warnings and penalties, respectively.

The optimal control model is outlined as follows:

$$\begin{cases} \frac{dS(t)}{dt}=rS(t)(1-\frac{S(t)}{K})-\frac{(1-p_1(t))\beta S(t)I(t)}{1+\alpha S(t)+\lambda I(t)}\\ \qquad -aS(t),\\ \frac{dI(t)}{dt}=\frac{(1-p_1(t-\tau_1))\beta e^{-m\tau_1}S(t-\tau_1)I(t-\tau_1)}{1+\alpha S(t-\tau_1)+\lambda I(t-\tau_1)}\\ \qquad -(b+k+p_2(t))I(t),\\ \frac{dH(t)}{dt}=kI(t)-(c+\eta)H(t)+\varepsilon e^{-m\tau_2}R(t-\tau_2),\\ \frac{dR(t)}{dt}=\eta H(t)-dR(t)-\varepsilon e^{-m\tau_2}R(t-\tau_2), \end{cases} \tag{22}$$

with the initial conditions

$$S(\theta)=\phi_1(\theta)\geq 0,\ I(\theta)=\phi_2(\theta)\geq 0,\ H(\theta)=\phi_3(\theta)\geq 0,$$

$$R(\theta)=\phi_4(\theta)\geq 0, \theta\in[-\tau_1,0],\ \phi_i(\theta)>0,\ (i=1,2,3,4).$$

First, we establish an optimal control problem. Let's assign a constant $\Im$ as the final implementation time of the control policy and define the control set $\mathcal{M}$:

$$\begin{aligned} \mathcal{M}=\{p=(p_1,p_2)|p_i(t)\text{ is Lebesgue measuralbe},\\ 0\leq p_i\leq p_i^{\max}, 0\leq t\leq\Im, i=1,2\}. \end{aligned} \tag{23}$$

Therefore, in order to minimize the total number of spreaders and related costs, we have the following optimal control function as follows.

$$\begin{aligned} \mathcal{Q}(S,I,H,R,p_1,p_2)=\int_0^{\Im}[\psi_1S(t)+\psi_2I(t)+\psi_3H(t)\\ +\frac{W_1}{2}p_1^2+\frac{W_2}{2}p_2^2]dt, \end{aligned} \tag{24}$$

where $\psi_1$, $\psi_2$, and $\psi_3$ balance the susceptible individuals and spreaders, while $W_1$ and $W_2$ are the weight parameters associated with the control variables $p_1$ and $p_2$. By [27], to find the optimal solution, we find the Hamiltonian of our optimal control problem (22) as given by

$$\begin{aligned} &\mathcal{J}(S,I,H,R,p_1,p_2)\\ &=\psi_1S(t)+\psi_2I(t)+\psi_3H(t)+\frac{W_1}{2}p_1^2+\frac{W_2}{2}p_2^2. \end{aligned} \tag{25}$$

And an augmented Hamiltonian function $\mathcal{U}$ for the inequality constrained Hamiltonian containing the control problem

$$\begin{aligned} &\mathcal{U}(S, I, H, R, p_1, p_2, \Upsilon_1, \Upsilon_2, \Upsilon_3, \Upsilon_4, t) \\ &= \psi_1 S(t) + \psi_2 I(t) + \psi_3 H(t) + \frac{W_1}{2} p_1^2 + \frac{W_2}{2} p_2^2 \\ &= \mathcal{J}(S, I, H, R, p_1, p_2) + \Upsilon_1 \frac{dS(t)}{dt} + \Upsilon_2 \frac{dI(t)}{dt} \\ &\quad + \Upsilon_3 \frac{dH(t)}{dt} + \Upsilon_4 \frac{dR(t)}{dt}. \end{aligned} \tag{26}$$

**Lemma 4.1** There exists an optimal pair $p^* = (p_1^*(t), p_2^*(t)) \in \mathcal{M}$ which minimizes the objective functional $\mathcal{Q}(S, I, H, R, p_1, p_2)$.

**Theorem 5.1** Let $(S^*, I^*, H^* R^*)$ be optimal state solution associated with the optimal control variables $p_1^*(t)$ and $p_2^*(t)$. Then, there must exist adjoint variables $\Upsilon_1,\ \Upsilon_2,\ \Upsilon_3$ and $\Upsilon_4$, satisfying

$$\begin{cases} \dfrac{d\Upsilon_1}{dt} = -\psi_1 - \Upsilon_1(t)(r - \dfrac{2rS^*}{K} - \varsigma_1) - \Re_{[0,\Im]} e^{-m\tau_1} \\ \qquad \times p_2(t+\tau_1)\varsigma_1, \\ \dfrac{d\Upsilon_2}{dt} = -\psi_2 + \Upsilon_1(t)\varsigma_2 + \Upsilon_2(b + k + p_2(t)) - \Upsilon_3 k \\ \qquad - \Re_{[0,\Im]} \Upsilon_2(t+\tau_1) e^{-m\tau_1} \varsigma_2, \\ \dfrac{d\Upsilon_3}{dt} = -\psi_3 + (c + \eta)\Upsilon_3, \\ \dfrac{d\Upsilon_4}{dt} = -\Upsilon_3 \varepsilon e^{-m\tau_2}. \end{cases} \tag{27}$$

where

$$\varsigma_1 = \frac{(1 - p_1(t))\beta I^*(1 + \lambda I^*)}{(1 + \alpha S^* + \lambda I^*)^2},$$

and

$$\varsigma_2 = \frac{(1 - p_1(t))\beta S^*(1 + \alpha S^*)}{(1 + \alpha S^* + \lambda I^*)^2}.$$

Therefore, under the boundary conditions $\Upsilon_i(\Im) = 0,\ (i = 1, 2, 3, 4)$, there exists an optimal control

$$\begin{aligned} p_1^* &= \max(\min(\frac{\Re_{[0,\Im]} e^{-m\tau_1} \Upsilon_2(t+\tau_1) - \Upsilon_1}{W_1(1 + \alpha S^* + \lambda I^*)} \beta S^* I^*, \\ &\quad p_1^{\max}),\ 0), 0 \le t \le \Im, \\ p_2^* &= \max(\min(\frac{\Upsilon_2 I^*}{W_2},\ p_2^{\max}),\ 0), \quad \text{otherwise}. \end{aligned} \tag{28}$$

**Proof** We define the Hamiltonian function as follows:

$$\begin{aligned} \mathcal{U}(t) &= \mathcal{J}(S, I, H, R, p_1, p_2) + \Upsilon_1 \frac{dS(t)}{dt} + \Upsilon_2 \frac{dI(t)}{dt} \\ &\quad + \Upsilon_3 \frac{dH(t)}{dt} + \Upsilon_4 \frac{dR(t)}{dt} \\ &= \psi_1 S(t) + \psi_2 I(t) + \psi_3 H(t) + \frac{W_1}{2} p_1^2 + \frac{W_2}{2} p_2^2 \\ &\quad + \Upsilon_1 (rS(1 - \frac{S}{K}) - aS - \frac{(1 - p_1(t))\beta S(t) I(t)}{1 + \alpha S(t) + \lambda I(t)}) \\ &\quad + \Upsilon_2 (\frac{(1 - p_1(t - \tau_1))\beta e^{-m\tau_1} S(t - \tau_1) I(t - \tau_1)}{1 + \alpha S(t - \tau_1) + \lambda I(t - \tau_1)} \\ &\quad - (b + k + p_2(t)) I(t)) + \Upsilon_3 (kI(t) - (c + \eta) H(t) \\ &\quad + \varepsilon e^{-m\tau_2} R(t - \tau_2)). \end{aligned} \tag{29}$$

Set $(S^*, I^*, H^*, R^*)$ is with the optimal control variable $p_1$ and $p_2$ related system (22) the optimal state variables. As per the Pontriagin maximum principle, the calculation of the partial derivative of the Hamiltonian function for each state yields adjoint variables $\Upsilon_1$, $\Upsilon_2$, $\Upsilon_3$, and $\Upsilon_4$ that satisfy the following equations:

$$\begin{cases} \dfrac{\Upsilon_1(t)}{dt} = -\dfrac{\partial \mathcal{U}}{\partial S} - \Re_{[0,\Im - \tau_1]} \dfrac{\mathcal{U}}{\partial S(t - \tau_1)}, \Upsilon_1(\Im) = 0, \\ \dfrac{\Upsilon_2(t)}{dt} = -\dfrac{\partial \mathcal{U}}{\partial I} - \Re_{[0,\Im - \tau_1]} \dfrac{\mathcal{U}}{\partial I(t - \tau_1)}, \Upsilon_2(\Im) = 0, \\ \dfrac{\Upsilon_3(t)}{dt} = -\dfrac{\partial \mathcal{U}}{\partial H} - \Re_{[0,\Im - \tau_1]} \dfrac{\mathcal{U}}{\partial H(t - \tau_1)}, \Upsilon_3(\Im) = 0, \\ \dfrac{\Upsilon_3(t)}{dt} = -\dfrac{\partial \mathcal{U}}{\partial R} - \Re_{[0,\Im - \tau_1]} \dfrac{\mathcal{U}}{\partial R(t - \tau_1)}, \Upsilon_4(\Im) = 0. \end{cases}$$

From the optimality condition $\frac{\partial \mathcal{U}}{\partial p_i} |_{S=S^*, I=I^*, H=H^*, R=R^*} = 0$, we obtain

$$\begin{cases} \dfrac{\partial \mathcal{U}}{\partial p_1} = W_1 p_1^* + \dfrac{\Upsilon_1 \beta S^* I^*}{1 + \alpha S^* + \lambda I^*} - \dfrac{\Upsilon_2(t+\tau_1)\beta S^* I^*}{1 + \alpha S^* + \lambda I^*} \\ \qquad \times \Re_{[0,\Im]} e^{-m\tau_1} = 0, \\ \dfrac{\partial \mathcal{U}}{\partial p_2} = W_2 p_2^* - \Upsilon_2 I^* = 0. \end{cases}$$

Thus, we obtain

$$p_1^* = \frac{\Re_{[0,\Im]} e^{-m\tau_1} \Upsilon_2(t+\tau_1) - \Upsilon_1}{W_1(1 + \alpha S^* + \lambda I^*)} \beta S^* I^*,\ p_2^* = \frac{\Upsilon_2 I^*}{W_2}.$$

Thus, by combining the properties of the control set (22), we obtain equations (28) and (29).

Based on the above results, we can find the optimal control pair and optimal state as follows:

$$\begin{cases} \dfrac{dS(t)}{dt} = rS(t)(1 - \dfrac{S(t)}{K}) - \dfrac{(1 - p_1(t))\beta S(t) I(t)}{1 + \alpha S(t) + \lambda I(t)} \\ \qquad - aS(t), \\ \dfrac{dI(t)}{dt} = \dfrac{(1 - p_1(t - \tau_1))\beta e^{-m\tau_1} S(t - \tau_1) I(t - \tau_1)}{1 + \alpha S(t - \tau_1) + \lambda I(t - \tau_1)} \\ \qquad - (b + k + p_2(t)) I(t), \\ \dfrac{dH(t)}{dt} = kI(t) - (c + \eta) H(t) + \varepsilon e^{-m\tau_2} R(t - \tau_2), \\ \dfrac{dR(t)}{dt} = \eta H(t) - dR(t) - \varepsilon e^{-m\tau_2} R(t - \tau_2), \\ \dfrac{d\Upsilon_1(t)}{dt} = -\psi_1 - \Upsilon_1(t)(r - \dfrac{2rS^*}{K} - \varsigma_1) - p_2(t+\tau_1)\varsigma_1 \\ \qquad \times \Re_{[0,\Im]} e^{-m\tau_1}, \\ \dfrac{d\Upsilon_2(t)}{dt} = -\psi_2 + \Upsilon_1(t)\varsigma_2 + \Upsilon_2(b + k + p_2(t)) - \Upsilon_3 k \\ \qquad - \Re_{[0,\Im]} \Upsilon_2(t+\tau_1) e^{-m\tau_1} \varsigma_2, \\ \dfrac{d\Upsilon_3(t)}{dt} = -\psi_3 + (c + \eta)\Upsilon_3, \\ \dfrac{d\Upsilon_4(t)}{dt} = -\Upsilon_3 \varepsilon e^{-m\tau_2}. \end{cases}$$

## VI. Numerical Examples

In this section, we will conduct numerical simulations to validate the findings of the previous theoretical analysis. We will provide a numerical representation of system (2) and examine the effects of two time delays on the system to support our analytical calculations.

### 6.1 The Effect of the Parameter $r$

In system (2), we utilized the parameters presented in Table 1 to examine how the parameter $r$ influences rumor diffusion.

Table 1: Description of all the system parameters

| Parameter and Description | Values |
|---|---|
| $\beta$ : The spreading rate | 1.4 |
| $\varepsilon$ : The questioning rate | 0.33 |
| $r$ : The population growth rate | $-$ |
| $K$: The environmental population capacity | 15 |
| $a$ : The emigration rate of the ignorant | 0.81 |
| $b$ : The migration rate of the spreader | 0.203 |
| $c$ : The immigration rate of the skeptics | 0.146 |
| $d$ : The emigration rate of the sober | 0.124 |
| $k$ : The rate at which individuals move from the spreading state to the questioning state | 0.62 |
| $\eta$ : The rate at which individuals move from the questioning state to the wakefulness state | 0.8 |
| $\tau_1$: The time delay for individuals to pass from hearing the rumor to the spread state | 0.85 |
| $\tau_2$: The time delay of the individual from questioning the rumor to the waking state | 1.88 |
| $\alpha$: Constant | 0.41 |
| $\lambda$: Constant | 0.15 |

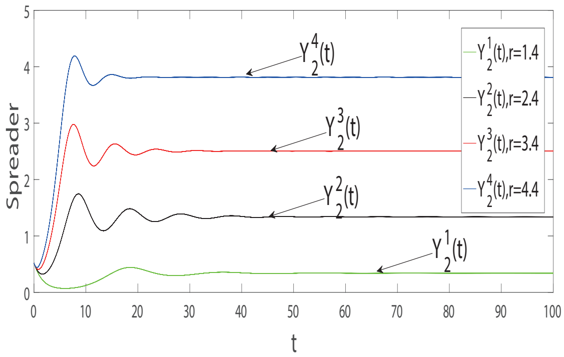


Figure 1. The path of I(t) under different $r$.

Where Figure 1 shows the stability of $I(t)$ when $r = 1.4,\ 2.4,\ 3.4$ and $4.4$.

**Remark 1.** Figure 1 indicates that the larger the $r$, the larger the peak value of the spreader. The population growth rate $r$ does not impact the stability of the system.

### 6.2 The Effect of the Parameter $\tau_1$ and $\tau_2$

We now explore the effect of the two delays on the number of spreaders. We consider the second set of parameters $\beta = 1.65, r = 2.4,\ a = 0.81, b = 0.203, c = 0.146, d = 0.124, k = 0.62,\ \eta = 0.8,\ \alpha = 0.41,\ \lambda = 0.15$.

First, we analyze the effect of time delay $\tau_2$ on the system.

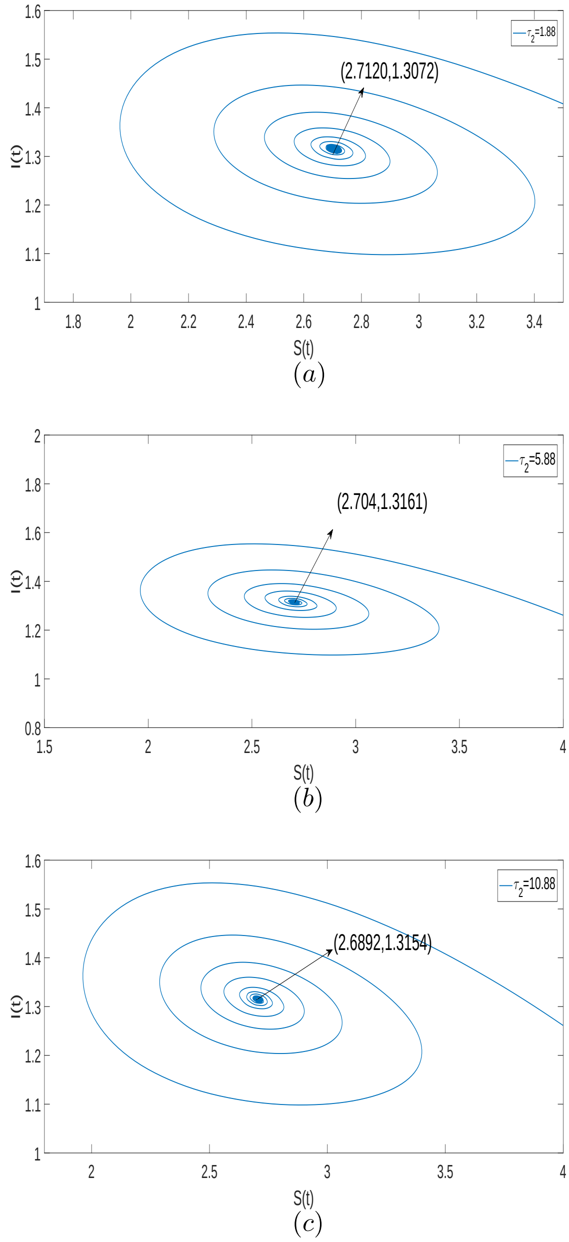


Figure 2. The effect of $\tau_2$ in system (2)

Where Figure 2(a), Figure 2(b) and Figure 2(c) show the stable planar phase diagram and the stable space phase diagram of $S(t),\ I(t)$ respectively when $\tau_2 = 1.88,\ 5.88,\ 10.88$.

**Remark 2.** Figure 2(a) and Figure 2(b) indicate that the peak value of the spread spectrum rises in accordance with the augmentation of the delay $\tau_2$. The time delay $\tau_2$ does not impact the stability of the system.

Next, consider the impact of $\tau_1$ on the system.

First, we demonstrate that when $\tau_1 = \tau_2 = 0$, the coexistence equilibrium $E_2$ of system (2) achieves a stable state without delay. The numerical results are presented in Figure 3. Under the assumption that $\tau_2 = 1.88$, system (2) allows the coexistence equilibrium $E_2$ to reach a steady state when $\tau_1 = 0$. Figures 4-6 present the corresponding value results. Through calculations, it is determined that $\tau_0 = 0.748$, indicating that a Hopf bifurcation occurs when system (2) meets the crossing condition at this value. When $\tau_1 = 0.056 < \tau_0$, system (2) becomes unstable at $E_2$, as shown in Figures 7-9. Conversely, when $\tau_1 = 0.8 > \tau_0$ is selected, system (2) is locally asymptotically stable at $E_2$, with the numerical results displayed in Figures 10-12. The correctness of Theorem 3.5 is verified based on the stability changes illustrated in Figures 4-12.

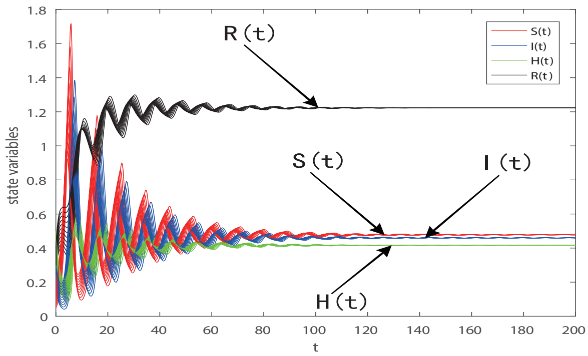


Figure 3. The time histories and the phase trajectories of system (2)

Finally, consider the phase diagram of system (2) with a rumor equilibrium point under the parameters in Table 1. where $\tau_1 = 0, \tau_2 = 1.88$. Directly from calculation, we get $R_0 = 8.1304 > 1$.From Figure 4, we observe that there is a rumor prevailing equilibrium point $E_2 \approx (0.6388, 0.1525, 0.1312, 0.6091)$ is globally asymptotically stable, which means the rumor will exist for a long tine. Figures 4 through 6 illustrate the corresponding simulation.

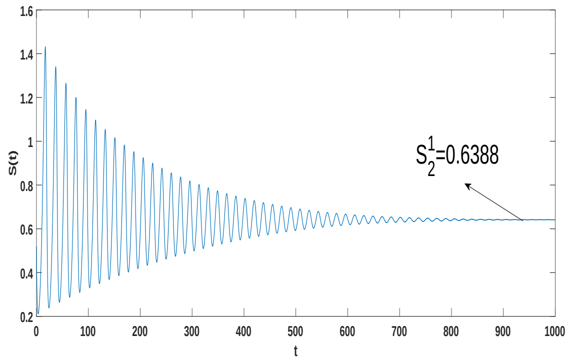


$(a)$

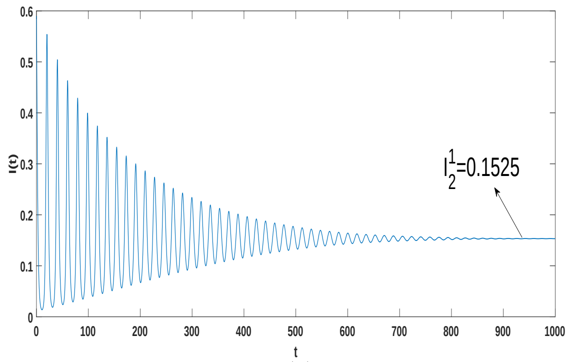


$(b)$

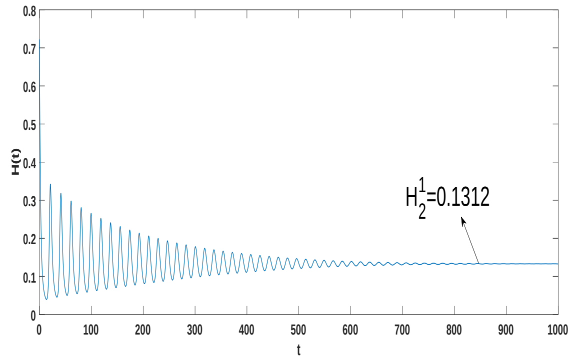


$(c)$

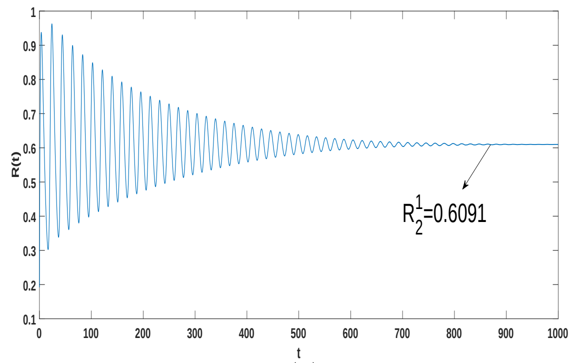


$(d)$

Figure 4. Waveform plots portraits of system (2) when $\tau_1 = 0, \ \tau_2 = 1.88$.

Where Figure $4(a)$ shows the stable time series diagram of $S(t)$. Figure $4(b)$ shows the stable time series diagram of $I(t)$. Figure $4(c)$ shows the stable time series diagram of $H(t)$. Figure $4(d)$ shows the stable time series diagram of $R(t)$.

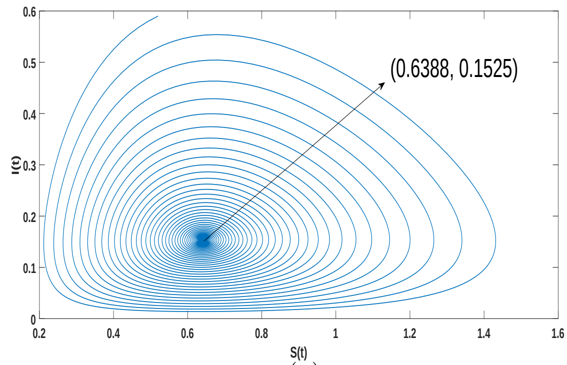


$(a)$

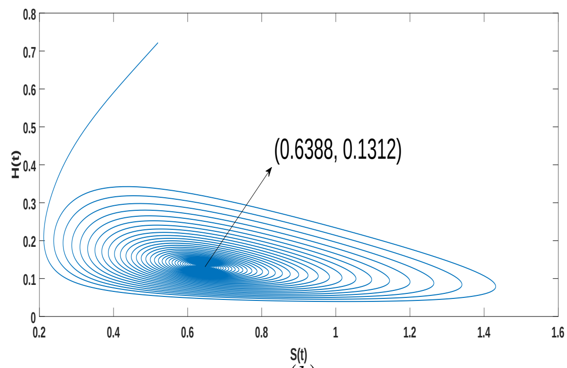


$(b)$

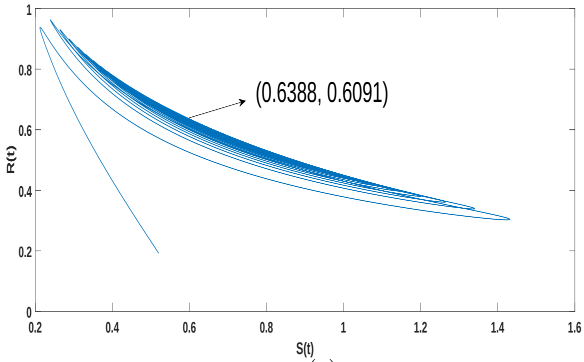


$(c)$

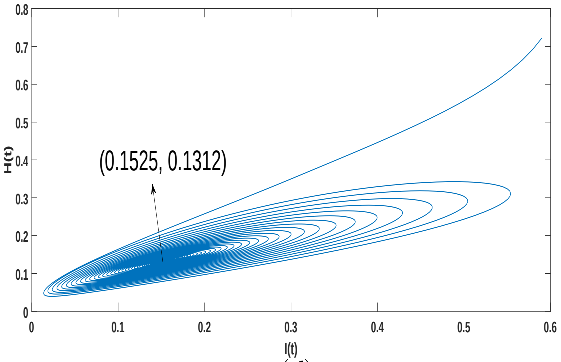


$(d)$

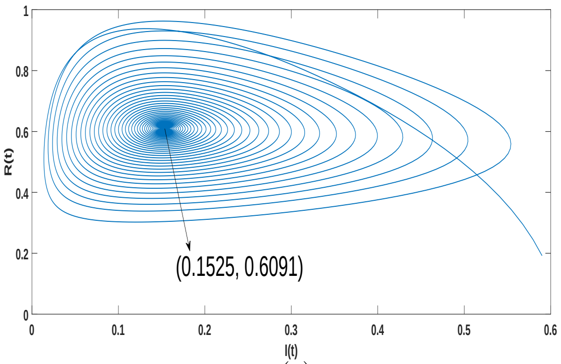


$(e)$

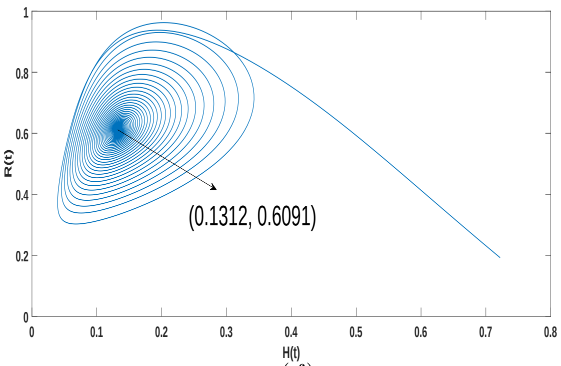


$(f)$

Figure 5. The two-dimension phase trajectories of system (2) when $\tau_1 = 0,\ \tau_2 = 1.88$.

Where Figure $5(a)$ shows stable planar phase diagram of $S(t)$ and $I(t)$. Figure $5(b)$ shows stable planar phase diagram of $S(t)$ and $H(t)$. Figure $5(c)$ shows stable planar phase diagram of $S(t)$ and $R(t)$. Figure $5(d)$ shows stable planar phase diagram of $I(t)$ and $R(t)$. Figure $5(e)$ shows stable planar phase diagram of $I(t)$ and $R(t)$. Figure $5(f)$ shows stable planar phase diagram of $H(t)$ and $R(t)$.

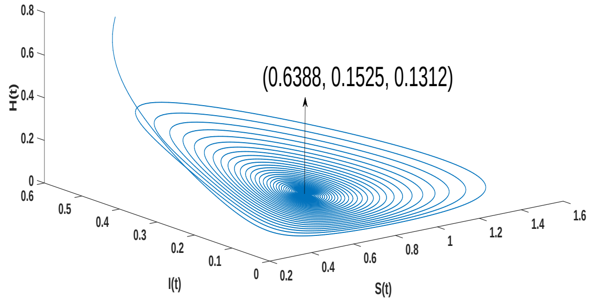


$(a)$

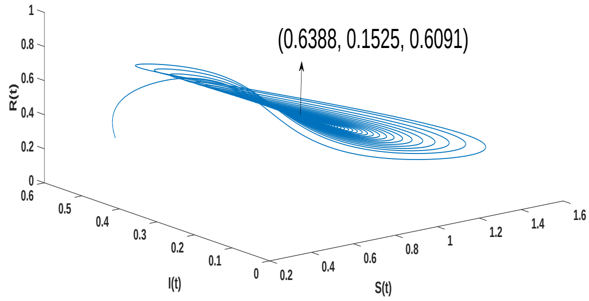


$(b)$

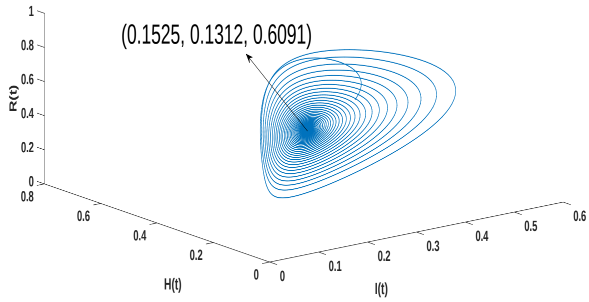


$(c)$

Figure 6. The three-dimension phase trajectories of system (2) when $\tau_1 = 0,\ \tau_2 = 1.88$.

Where Figure $6(a)$ shows stable space phase diagram of $S(t),\ I(t)$ and $H(t)$. Figure $6(b)$ shows stable space phase diagram of $S(t),\ I(t)$ and $R(t)$. Figure $6(c)$ shows stable space phase diagram of $I(t),\ H(t)$ and $R(t)$.

In system (2), if we take $\tau_1 = 0.056,\ \tau_2 = 1.88$, then we have $R_0 = 7.6876 > 1$. Figures 7 through 9 illustrate the corresponding simulation.

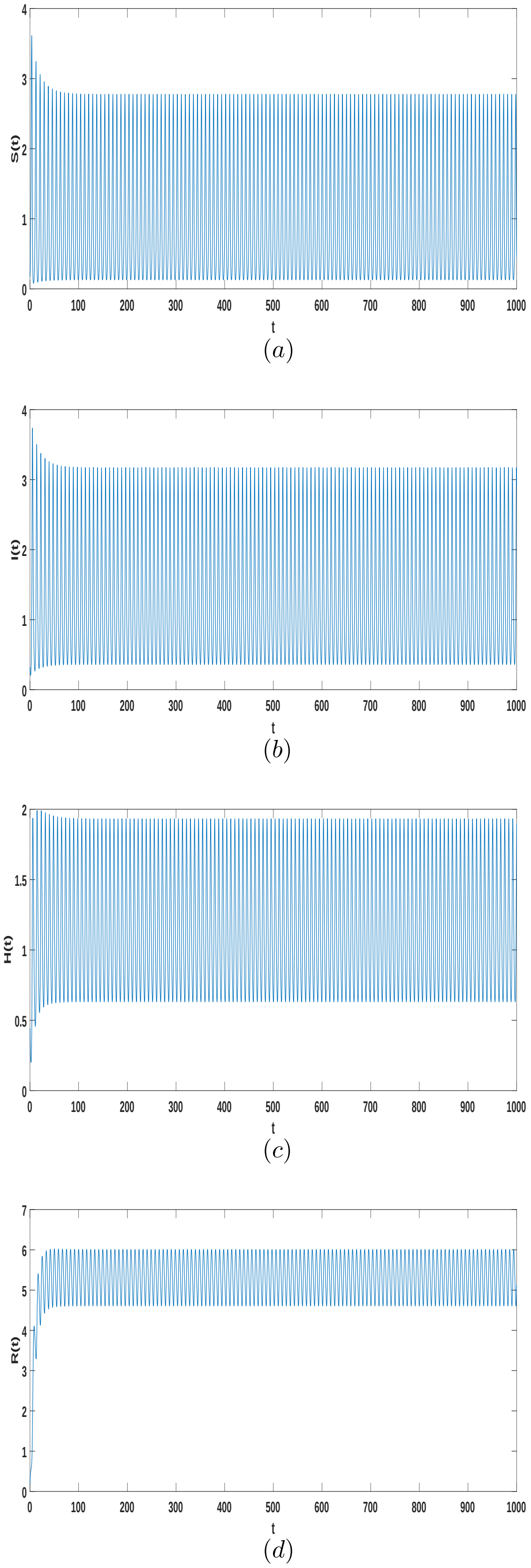


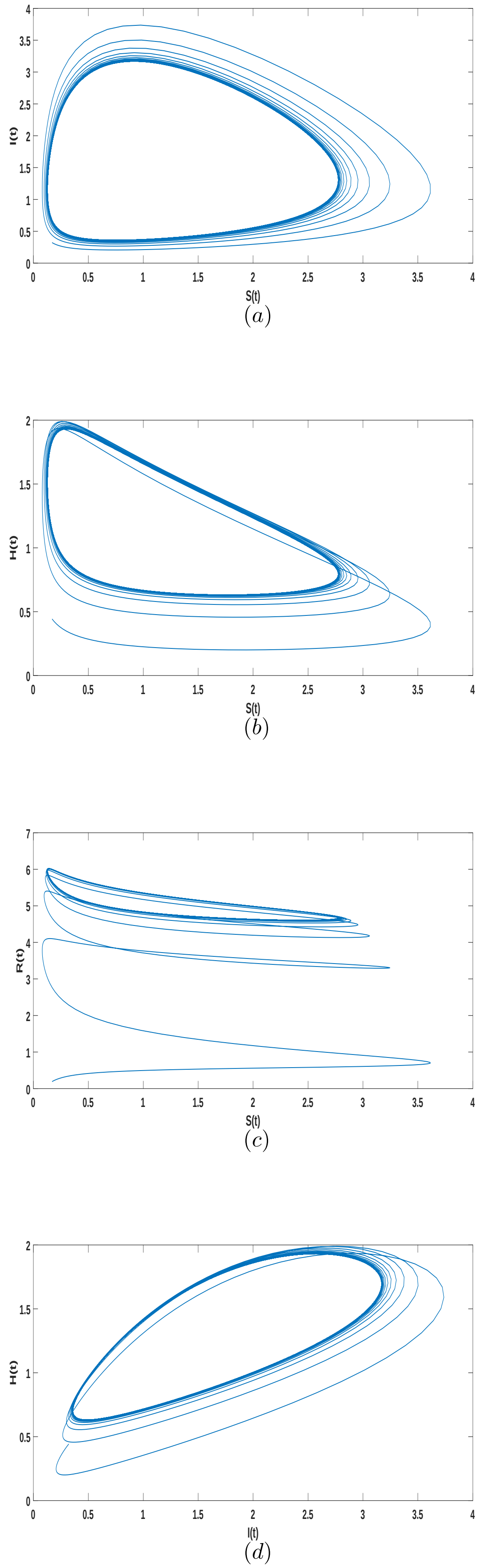


Figure 7. Waveform plots and phase portraits of system (2) when $\tau_1 = 0.056$ and $\tau_2 = 1.88$.

Where Figure 7$(a)$ show unstable time series diagram of $S(t)$. Figure 7$(b)$ shows unstable time series diagram of $I(t)$. Figure 7$(c)$ shows unstable time series diagram of $H(t)$. Figure 7$(d)$ shows unstable time series diagram of $R(t)$.

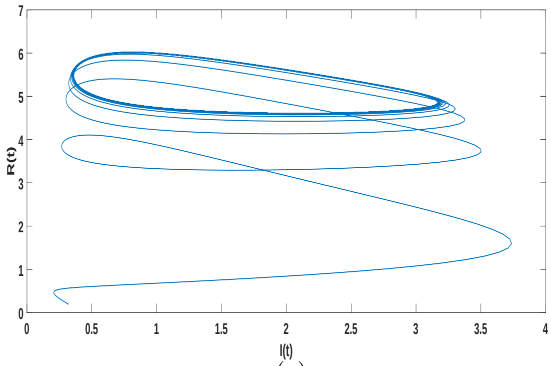


$(e)$

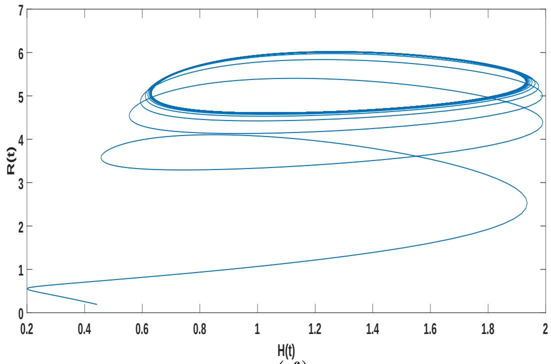


$(f)$

Figure 8. The two-dimension phase trajectories of system (2) when $\tau_1 = 0.056$ and $\tau_2 = 1.88$.

Where Figure 8$(a)$ shows unstable planar phase diagram of $S(t)$ and $I(t)$. Figure 8$(b)$ shows unstable planar phase diagram of $S(t)$ and $H(t)$. Figure 8$(c)$ shows unstable planar phase diagram of $S(t)$ and $R(t)$. Figure 8$(d)$ shows unstable planar phase diagram of $I(t)$ and $H(t)$. Figure 8$(e)$ shows unstable planar phase diagram of $I(t)$ and $R(t)$. Figure 8$(f)$ shows unstable planar phase diagram of $H(t)$ and $R(t)$.

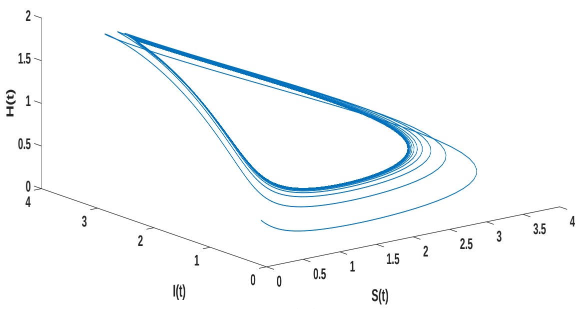


$(a)$

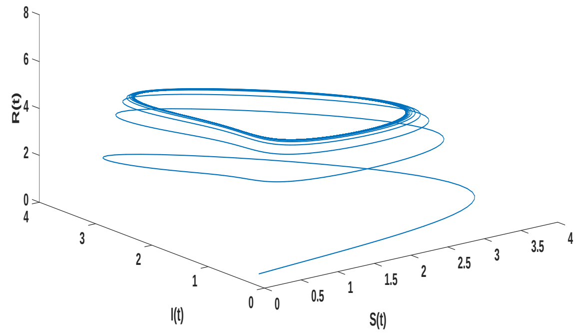


$(b)$

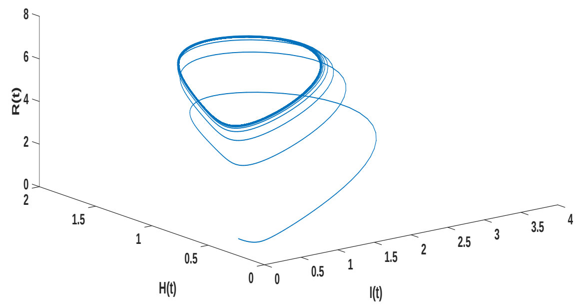


$(c)$

Figure 9. The three-dimension phase trajectories of system (2) when $\tau_1 = 0.056$ and $\tau_2 = 1.88$.

Where Figure 9$(a)$ shows unstable space phase diagram of $S(t)$, $I(t)$ and $H(t)$. Figure 9$(b)$ shows unstable space phase diagram of $S(t)$, $I(t)$ and $R(t)$. Figure 9$(c)$ shows unstable space phase diagram of $I(t)$, $H(t)$ and $R(t)$.

In system (2), if we take $\tau_1 = 0.8$, $\tau_2 = 1.88$, then we have $R_0 = 3.6532 > 1, E_2 \approx (2.082, 0.1403, 0.1202, 0.5502)$. Figures 10 through 12 illustrate the corresponding simulation.

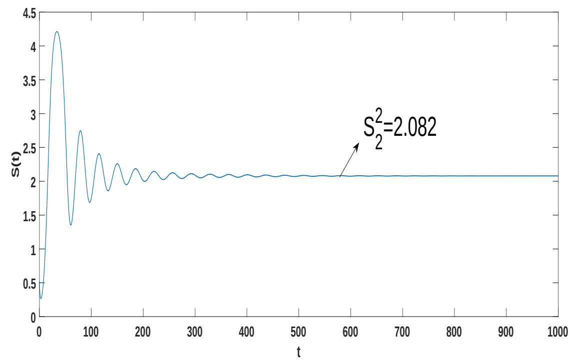


$(a)$

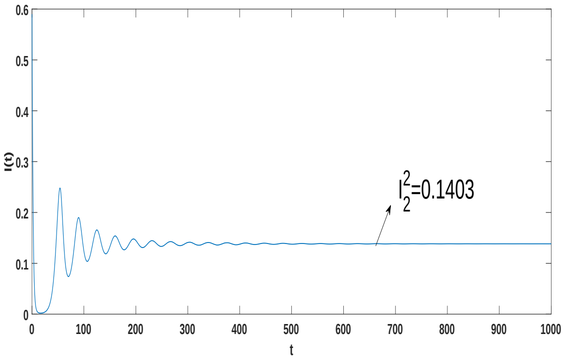


$(b)$

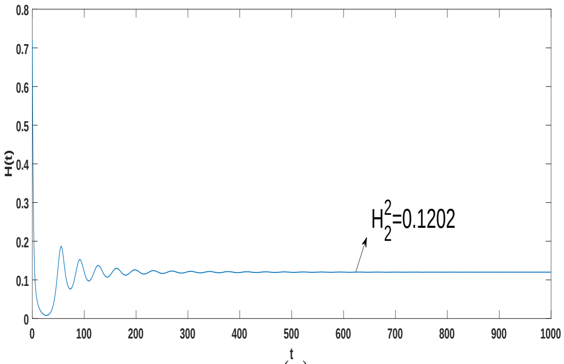


$(c)$

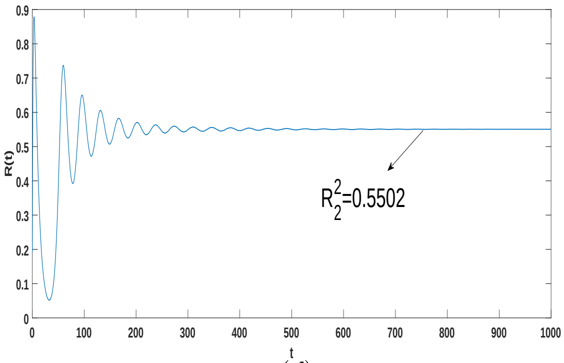


$(d)$

Figure 10. The time histories of system (2) when $\tau_1 = 0.8$, $\tau_2 = 1.88$.

Where Figure 10$(a)$ shows stable time series diagram of $S(t)$. Figure 10$(b)$ shows stable time series diagram of $I(t)$. Figure 10$(c)$ shows stable time series diagram of $H(t)$. Figure 10$(d)$ shows stable time series diagram of $R(t)$.

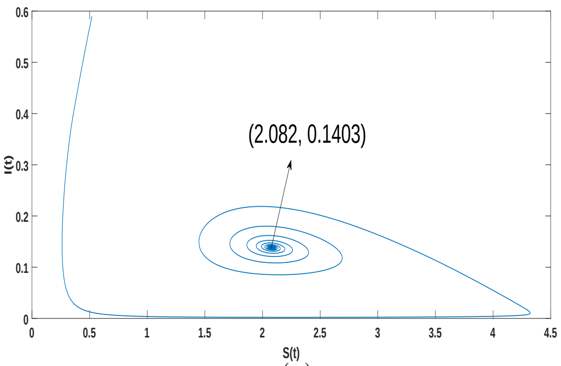


$(a)$

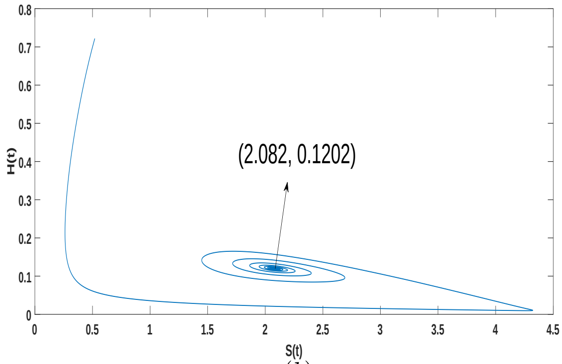


$(b)$

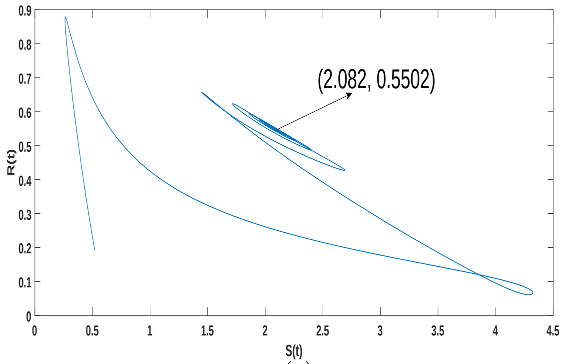


$(c)$

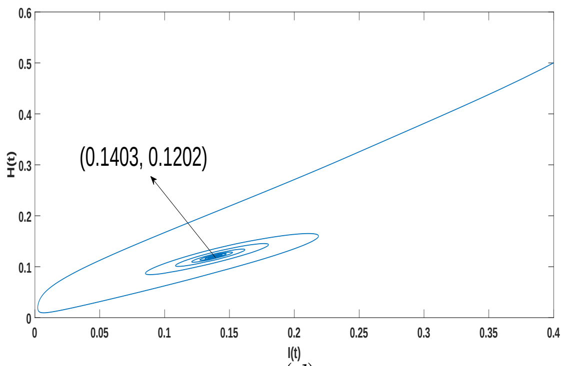


$(d)$

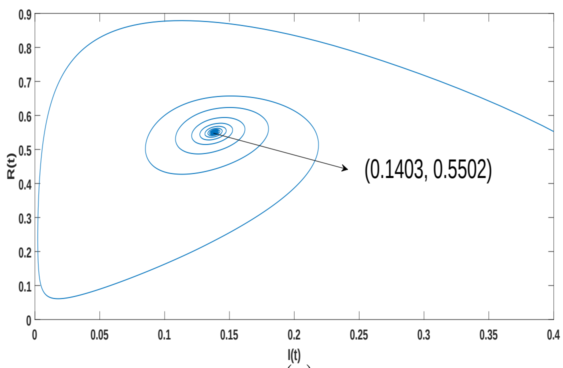


$(e)$

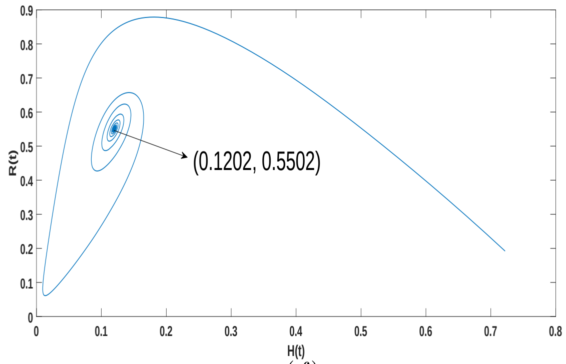


$(f)$

Figure 11. The two-dimension phase trajectories of system (2) when $\tau_1 = 0.8$, $\tau_2 = 1.88$.

Where Figure 11$(a)$ show stable planar phase diagram of $S(t)$ and $I(t)$. Figure 11$(b)$ show stable planar phase diagram of $S(t)$ and $H(t)$. Figure 11$(c)$ shows stable planar phase diagram of $S(t)$ and $R(t)$. Figure 11$(d)$ shows stable planar phase diagram of $I(t)$ and $R(t)$. Figure 11$(e)$ shows stable planar phase diagram of $I(t)$ and $R(t)$. Figure 11$(f)$ shows stable planar phase diagram of $H(t)$ and $R(t)$.

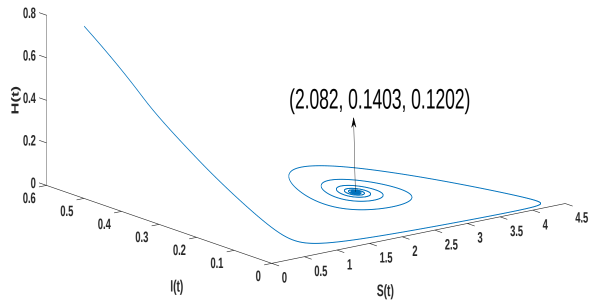


$(a)$

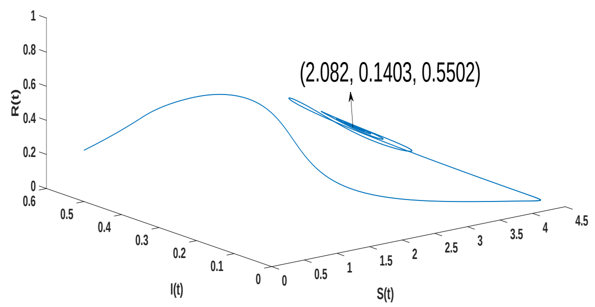


$(b)$

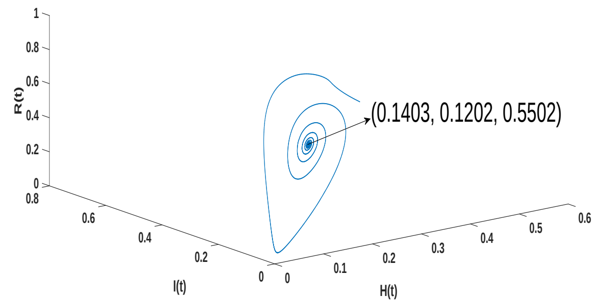


$(c)$

Figure 12. The three-dimension phase trajectories of system (2) when $\tau_1 = 0.8$, $\tau_2 = 1.88$.

Where Figure 12$(a)$ shows stable space phase diagram of $S(t)$, $I(t)$ and $H(t)$. Figure 12$(b)$ shows stable space phase diagram of $S(t)$, $I(t)$ and $R(t)$. Figure 12$(c)$ shows stable space phase diagram of $I(t)$, $H(t)$ and $R(t)$.

From Figures 2-12, it is evident that $\tau_1$ has a significant effect on the stability and existence of system branches. However, $\tau_2$ has minimal influence on the system. Thus, the numerical simulation suggests that to control the development of rumors, it is more effective to regulate the number of spreaders or delay in propagation time during the rumor transmission process. In contrast, controlling the time individuals spend on refuting rumors has a negligible impact on the system, especially for those who are skeptical.

## VI. Conclusions

In this study, we considered a delayed rumor propagation model based on logistic growth and Beddington-DeAngelis functional responses, that is, Model (2). The existence, non-negativity, persistence, and boundedness of the model solutions were proved. We set up conditions under which a rumor equilibrium exists. By constructing the Lyapunov function, the global stability of the rumourless equilibrium and rumourless equilibrium are studied, and the local stability and Hopf bifurcation caused by the time delay are analyzed. Finally, the numerical simulation shows that the time delay of $\tau_1$ is a sensitive factor affecting the system performance and leads to Hopf bifurcation. The theoretical results and model (2) in this study can be regarded as an extension and supplement to the existing theoretical results and models.

In the time-delay model, two control strategies are introduced to address the proliferation of misinformation. The first involves removing posts from platforms that propagate rumors, thereby eradicating rumor-related content and minimizing the exposure of uninformed individuals to such misinformation. The second strategy entails educating individuals with limited knowledge of popular science topics, enabling them to differentiate between real information and rumors more easily. This approach not only disseminates accurate information but also empowers individuals to become critical thinkers, potentially decreasing the spread of misinformation in the system.

## References

[1] DJ. Daley, DG. Kendall, "Epidemics and rumours",*Nature*, vol. 204, no. 4963, pp. 1118-1118, 1964.

[2] DP. Maki, M. Thompson, “Mathematical Models and Applications”, *Prentice-Hall, Englewood Cliffs (NJ)*, 1973.
[3] L. Zhu, M. Liu, Li. Yimin, “The dynamics analysis of a rumor prop agation model in online social networks”, *Physica A: Statistical Mechanics and its Applications*, vol. 520, pp. 118-137, 2019.
[4] Z. Yu, S. Lu, D Wang, “Modeling and analysis of rumor propagation in social networks”, Information Sciences, vol. 580, pp. 857-873, 2021.
[5] L. Zhao, H. Cui, X. Qiu, “SIR rumor spreading model in the new med ia age”, *Physica A: Statistical Mechanics and its Applications*, vol. 392, no. 4, pp. 995-1003.
[6] L. Zhao, J. Wang, “SIHR rumor spreading model in social networks”, *Physica A: Statistical Mechanics and its Applications*, vol. 391, no. 7, pp. 2444-2453, 2012.
[7] L. Zhu, X. Zhou, Y. Li, “Global dynamics analysis and control of a rumor spreading model in online social networks”, *Physica A: Statistical Mechanics and its Applications*, vol. 526, pp. 120903, 2019.
[8] R. Yin, A. Muhammadhaji, “Dynamics in a delayed rumor propagation model with logistic growth and saturation incidence”, *AIMS Mathematics*, vol. 9, no. 2, pp. 4962-4989, 2024.
[9] Y. Zhang, Z. Chen, “SETQR propagation model for social networks”, *IEEE Access*, vol. 7, pp. 127533-127543. 2019
[10] S. Shen, X. Ma, L. Zhu, “Bifurcation dynamical analysis of an epidemic-like SIR propagation model with Logistic growth”, *The European Physical Journal Plus*, vol. 138, no.10, pp. 934, 2023.
[11] L. Zhao, H. Cui, “SIR rumor spreading model in the new media age”, *Physica A: Statistical Mechanics and its Applications*, vol. 392, no. 4, pp. 995-1003, 2013.
[12] H. Zhao, L. Zhu, “Dynamic analysis of a reaction-diffusion rumor propagation model diffusion rumor propagation model”, *International Journal of Bifurcation and Chaos*, vol. 26, no. 6, pp. 1650101, 2016.
[13] M. Ghosh, S. Das, P. Das, “Persistence of delayed cooperative models: Impulsive control method”, *Applied Mathematics and Computation*, vol. 68, pp. 3011-3040, 2022.
[14] L. Zhu, X. Huang, “SIS model of rumor spreading in social network with time delay and nonlinear functions”, *Communications in Theoretical Physics*, vol. 72, no. 1, pp. 015002, 2019.
[15] H. Laarabi, A. Abta, M. Rachik, “Stability analysis of a delayed rumor propagation ”, *Differential Equations and Dynamical System*, vol. 24, pp. 407-415, 2016.
[16] L. Zhu, X. Wang, Z. Zhang, “Global stability and bifurcation analysis of a rumor propagation model with two discrete delays in social networks”, *International Journal of Bifurcation and Chaos*, vol. 30, no. 12, pp. 2050175, 2020.
[17] H. Guo, X. Yan, Y. Niu, “Dynamic analysis of rumor propagation model with media report and time delay on social networks”, *Journal of Applied Mathematics and Computing*, vol. 69, no. 3, pp. 2473-2502, 2023.
[18] C. Li, Z. Ma, “Dynamics analysis and optimal control for a delayed rumor-spreading model”, *Mathematics*, vol. 10, no. 19, pp. 3455, 2022.
[19] D. Li, Y. Zhao, Y. Deng, “Rumor spreading model with a focus on educational impact and optimal control”, *Nonlinear Dynamics*, vol. 112, no. 2, pp. 1575-1597, 2024.
[20] A. Jian, J. Dhar, VK. Gupta, “Optimal control of rumor spreading model on homogeneous social network with consideration of influence delay of thinkers”, *Journal of the Egyptian Mathematical Society*, vol. 31, no.1, pp. 113-134, 2023.
[21] H. Miao, C. Kang,“ Stability and Hopf bifurcation analysis for an HIV infection model with Beddington-DeAngelis incidence and two de lays”, *Journal of Applied Mathematics and Computing*, vol. 60, pp. 265-290, 2019.
[22] JR. Beddington, “Mutual interference between parasites or predators and its effect on searching efficiency”, *The Journal of Animal Ecology*, pp. 331-340, 1975.
[23] DL. DeAngelis, RA. Goldstein, RV. O’Neill, “A model for tropic interaction”, *Journal of Differential Equations*, vol.56, no. 4, pp. 881-892, 1975.
[24] JK. Hale, S. Lunel, “Introduction to Functional Differential Equations”, *Springer, New York*, 1993.
[25] J. Hale, P. Waltman, “Persistence in infinite-dimensional systems”, *SIAM Journal on Mathematical Analysis*, vol.20, pp. 388-395,1989.
[26] XQ. Zhao, “Dynamical systems in population biology”, *Springer, New York*, 2003.
[27] G. Huang, W. Ma, Y. Takeuchi, “Global properties for virus dynamics model with Beddington-DeAngelis function response”, *Applied Mathematics Letters*, vol.22 , pp. 1690-1693, 2009.
[28] G. Huang, W. Ma, Y. Takeuchi, “Global analysis for delay vir us dynamics model with Beddington-DeAngelis function response”, *Applied Mathematics Letters*, vol. 24, pp. 1199-1203, 2011.